Wilfred C. G. Peh
Editor

Pitfalls in Musculoskeletal Radiology

Springer

Pitfalls in Musculoskeletal Radiology

Wilfred C.G. Peh
Editor

Pitfalls in Musculoskeletal Radiology

Springer

Editor
Wilfred C.G. Peh, MD, FRCP (Edin), FRCP (Glasg), FRCR
Department of Diagnostic Radiology
Khoo Teck Puat Hospital
Singapore
Republic of Singapore

ISBN 978-3-319-53494-7 ISBN 978-3-319-53496-1 (eBook)
DOI 10.1007/978-3-319-53496-1

Library of Congress Control Number: 2017941712

Printed on acid-free paper

This Springer imprint is published by Springer Nature
The registered company is Springer International Publishing AG
The registered company address is: Gewerbestrasse 11, 6330 Cham, Switzerland

Foreword

I am honored to be able to write a foreword for this new and timely book *Pitfalls in Musculoskeletal Radiology*, edited by my good friend, Wilfred Peh, with a contributing cast that includes many of the distinguished members of the International Skeletal Society. I am very familiar with the time commitment and hard work that the preparation of such books involves, having myself been involved with the publication of books in the past. Although Wilfred suggests that his task was simple, merely "conceptualizing the contents of this book and then approaching these friends to contribute their considerable expertise," I know for fact that it takes a motivated and knowledgeable editor to determine what subjects need to be addressed and who specifically would be the correct person or persons to complete the work. Clearly, it helps if that editor has a worldwide reputation as an educator with the ability to identify the right people and obtain their approval as contributors. The result is a book that is desperately needed and will become an instant success.

There are countless texts currently available that cover the spectrum of musculoskeletal imaging in a variety of disorders, but there is none that emphasizes those pitfalls that cause confusion in image interpretation and misdiagnosis. Such pitfalls include many anatomic variants and technique-specific artifacts, and they are encountered every day in clinical practice. I myself have struggled with these throughout my career and, until now, had no single place to go to figure out with what I was dealing. Now I do. Indeed, in the pages of this book can be found reference to pitfalls in conventional radiography, ultrasonography, computed tomography, magnetic resonance, nuclear medicine, arthrography, and interventional procedures, with information collected and detailed by experts in each one of these modalities and techniques. General, disease-specific, and regional-specific artifacts and variants are covered, with succinct and clear writing, vivid illustrations, and pertinent references for further reading. Each chapter is well organized and a pleasure to read, providing useful information that will allow the reader to avoid mistakes in interpretation that otherwise would occur daily.

Wilfred Peh is not new to book-writing. His impressive resume confirms a lifelong commitment to education. His previous texts have all been well received. But *Pitfalls in Musculoskeletal Radiology* will likely turn out to be the most successful of the lot, because this book addresses a subject that has been largely ignored and one that has a great clinical impact. Purchase this

book, place it at an easily accessible spot on your desk or shelf, and refer to it often and I can guarantee that you will become better in the interpretation of imaging studies related to the musculoskeletal system. Congratulations Wilfred and contributors (many of whom are friends of mine), this is a job well done! I am privileged to be able to write this foreword.

San Diego, USA
30 July 2016

Donald Resnick, MD

Preface

The growing applications of advanced imaging modalities such as high-resolution ultrasound (US) imaging, dual-energy computed tomography, and magnetic resonance imaging (MRI) have made the daily clinical practice of musculoskeletal radiology progressively complex. While these modalities can show a larger number of musculoskeletal structures in greater detail, with more sensitivity and higher resolution, they may also result in the production of technique-specific artifacts and the detection of unsuspected anatomical variants. Failure to recognize these imaging artifacts and variants may lead to diagnostic error and misinterpretation, with resultant medicolegal implications.

Potentially correctable pitfalls may also result from inadequate imaging technique, lack of training/inexperience, and failure to correlate with other imaging findings, in particular radiographs. Pitfalls in imaging interpretation also occur during imaging of trauma to structures such as bones, joints, tendons, ligaments, and muscles, in different regions of the musculoskeletal system at different ages, as well as various diseases affecting these structures, such as inflammatory arthritides, infections, metabolic bone lesions, congenital skeletal dysplasias, tumors, and tumorlike conditions. Recognition of these pitfalls is crucial in helping the practicing radiologist achieve a more accurate diagnosis. However, it is increasingly difficult for musculoskeletal radiologists, let alone general radiologists and residents, to know all of these pitfalls. This textbook aims at highlighting the spectrum of pitfalls that may occur in musculoskeletal radiology and, where possible, provides suggestions for overcoming or avoiding these pitfalls.

This book came about as I was nearing the tail end of completing the well-received *Pitfalls in Diagnostic Radiology*, published by Springer-Verlag (Berlin/Heidelberg) in 2015. As with the previous book project, I sounded out the idea for *Pitfalls in Musculoskeletal Radiology* to my good friend, Dr. Ute Heilmann, editorial director of clinical medicine at Springer-Verlag, who replied within days saying "Again a very promising project from you!....I am confident that under your leadership, a sound project, worthwhile to be published and of value to the community." I once again thank Ute, for her decisive and complete support, and her staff, for competently managing this project.

This book addresses a topic very close to my heart and also to the hearts of many of my musculoskeletal radiologist friends, the majority of whom are distinguished members of the International Skeletal Society. Hence, I was left

with the relatively simple task of conceptualizing the contents of this book and then approaching these friends to contribute their considerable expertise. The resultant *Pitfalls in Musculoskeletal Radiology* highlights musculoskeletal imaging pitfalls in a comprehensive and systematic manner and draws on the vast collective experiences of an international group of 97 radiologists from 51 reputable centers in 18 countries located in different parts of the world – as far as I know, the only such book available. To my willing author friends, I give my sincere thanks.

The resultant book consists of 43 chapters, well illustrated with 892 figures and 1,585 individual images. As with *Pitfalls in Diagnostic Radiology*, I have tried to edit the contributions of these experts with a light touch so as to retain, as much as possible, the original flow of each chapter according to the diverse experiences and perspectives of each author. Some overlap among chapters will be inevitable but not necessarily a bad thing. For example, the magic angle phenomenon is first explained in Chap. 4 on MRI artifacts but is also highlighted in chapters on MRI pitfalls of shoulder injury (Chap. 15), elbow injury (Chap. 17), wrist and hand injuries (Chap. 19), and cartilage imaging (Chap. 40), among others. In a similar vein, the anisotropy artifact appears in Chap. 2 on US imaging artifacts, as well as in chapters dealing with US pitfalls of injuries to the shoulder (Chap. 16), elbow (Chap. 18), and hip (Chap. 22). Discussion of diagnostic pitfalls in these individual chapters would not have been complete without a mention of these two artifacts. Similarly, marrow reconversion is relevant in topics as diverse as elbow injury (Chap. 17), knee injury (Chap. 23), treated musculoskeletal tumors (Chap. 32), multifocal and multisystemic bone lesions (Chap. 36), hematological and circulatory bone conditions (Chap. 37), and pediatric lesions (Chap. 38).

My grateful thanks go to my good friend and role model Professor Donald Resnick, who graciously wrote the foreword for this book.

Pitfalls in Musculoskeletal Radiology is dedicated to my dearest mother, Libby Tin Peh. She is the best mother that any son can wish for and is the most wonderful human being.

Singapore
31 December 2016

Wilfred C.G. Peh

Contents

Part I

Imaging Modality and Technique Pitfalls Related to the Musculoskeletal System

Radiography Limitations and Pitfalls

1

Keynes T.A. Low and Wilfred C.G. Peh

Contents

K.T.A. Low, MBBS, MMed, FRCR
W.C.G. Peh, MD, FRCPE, FRCPG, FRCR (✉)
Department of Diagnostic Radiology,
Khoo Teck Puat Hospital, 90 Yishun Central,
Singapore 768828,
Republic of Singapore
e-mail: low.keynes.ta@alexandrahealth.com.sg;
wilfred.peh@alexandrahealth.com.sg

Abbreviations

ALARA	As low as reasonably achievable
CT	Computed tomography
MRI	Magnetic resonance imaging
US	Ultrasound

1.1 Introduction

It is widely acknowledged that radiography should be the initial imaging modality in the evaluation of most suspected musculoskeletal lesions. They are often adequate for diagnosis, although advanced imaging modalities such as computed tomography (CT) and magnetic resonance imaging (MRI) are still often required for more detailed assessment of structures such as bone marrow and various soft tissues. Nevertheless, radiographs play an important complementary role to these newer cross-sectional imaging techniques. For example, they can provide a big picture view of bony or joint abnormalities, which allows better assessment of conditions such as the inflammatory arthritides (e.g., by showing distribution and pattern of joint involvement). Radiographs can also demonstrate calcifications and ossifications, which might not be convincingly seen on MRI. In fact, radiography still remains the most specific imaging modality for the diagnosis of bone tumors.

Radiographs are commonly obtained for acute musculoskeletal trauma, infection, chronic arthropathies, and bone or soft tissue tumors. They are also performed for follow-up imaging after treatment

W.C.G. Peh (ed.), *Pitfalls in Musculoskeletal Radiology*, DOI 10.1007/978-3-319-53496-1_1

such as fracture fixation and joint replacement. Radiographs are widely available, inexpensive, and well tolerated and can be rapidly and easily obtained. As with any imaging modality, radiography has advantages and disadvantages. Radiographs are of limited value in the evaluation of soft tissue injuries, for example, musculotendinous, cartilaginous, or ligamentous injuries. These soft tissue structures are not clearly seen on the radiograph and are better assessed on MRI or ultrasound (US) imaging, both of which have superior soft tissue resolution. Radiography is also limited in the assessment of conditions such as osteomyelitis and non-displaced acute fractures, both of which can be radiographically occult. Certain scenarios make it challenging or impossible to accurately interpret radiographs, for example, when an external cast obscures bone or when a background of osteopenia results in a paucity of osseous detail. Apart from the aforementioned intrinsic limitations of the radiographic modality, other potential pitfalls in relation to radiographic technique can be encountered. Proper positioning of the patient is crucial in obtaining a radiograph of diagnostic quality. An adequate coverage of the area of interest and an adequate number of views are also necessary for proper evaluation.

1.2 Pitfalls Related to Radiographic Image Acquisition

Radiography is often the initial modality used in the imaging workup of patients with musculoskeletal complaints. It is the workhorse in the emergency department, where it is able to support the high patient throughput. Despite the time pressure, the radiographer has to be meticulous during the acquisition of radiographs as a multitude of potential pitfalls may occur, limiting the accuracy of the evaluation and ultimately negatively impacting upon the clinical management of patients.

1.2.1 Adequacy of Coverage and Views

When radiographic imaging is requested, one of the fundamental responsibilities of the radiologist is to ensure adequate coverage and sufficient views of the anatomical region of interest. For example, a full radiographic series of the cervical spine should include an anteroposterior view, a lateral view, and an open-mouth odontoid view. On the lateral view, the entire cervical spine should be visualized with the base of the skull seen superiorly and the cervicothoracic junction (C7-T1 level) seen inferiorly. If the routine lateral view is insufficient, attempts should be made to better visualize the cervicothoracic junction (e.g., performing a swimmer's view) (Fig. 1.1). Missing a significant injury as a result of inadequate coverage on imaging evaluation is virtually indefensible in the court of law. The example of the cervical spine radiograph is particularly pertinent due to the medicolegal implications of a missed unstable cervical spine injury, which can result in devastating neurological sequelae. CT has been shown to have superior sensitivity and has largely superseded radiography in the detection of cervical spine injuries in patients who have high risk of injury (Holmes and Akkinepalli 2005). Obtaining high-quality radiographs with adequate coverage tends to be challenging in these patients due to difficulties in positioning. However, radiography is still used for screening low-risk patients with an indication for imaging, and adequate coverage of anatomy remains crucial.

Another potential pitfall is the failure to cover separate associated anatomical regions which may be involved while imaging the primary area of interest. For example, in a patient with injury to the medial ankle structures, a Maisonneuve injury may be missed if imaging does not include the proximal fibula (Pankovich 1976) (Fig. 1.2). Associated injuries should be suspected based on the injury mechanism and the imaging of the relevant area obtained, if indicated. In another example, a calcaneal fracture is usually due to an axial loading force and should raise the suspicion of spinal injury, especially at the thoracolumbar junction.

In general, orthogonal views are sufficient in the radiographic imaging of the axial and appendicular skeleton (Fig. 1.3). However, additional views may be required based on the complexity of the anatomy, especially if the structure of

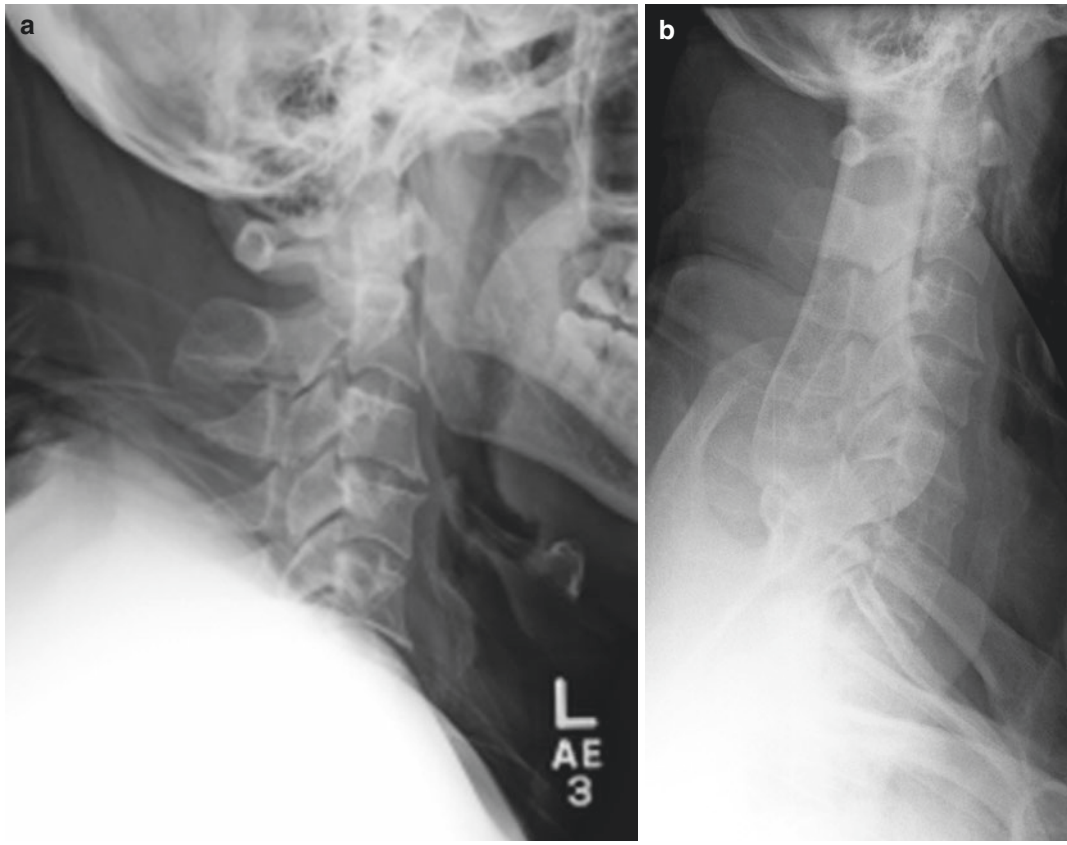

Fig. 1.1 A 47-year-old man who presented with neck pain following a motor vehicle accident. (**a**) Lateral radiograph of the cervical spine shows inadequate coverage of anatomy. The cervical spine inferior to the C5 level, as well as the cervicothoracic junction, is obscured by the shoulder girdle. (**b**) A swimmer's view was performed as a complementary study and ensured complete coverage of the region of interest

interest has a complex shape. Recognition that there are insufficient views can help to identify this pitfall and prevent potential missed diagnoses. In the knee, for example, a skyline view may demonstrate an avulsion fracture of the medial aspect of the patella in relation to transient patellar dislocation (Fig. 1.4). This finding would have been missed on routine anteroposterior and lateral views of the knee. In the case of the scaphoid bone, the standard posteroanterior and lateral radiographs of the wrist are usually insufficient for this complex-shaped bone, with additional views needed for adequate evaluation. Although previous studies show varying recommendations on the number and specific views required in the scaphoid series, a posteroanterior view of the wrist with ulnar deviation and slight tube angulation is usually part of the imaging series (Malik et al. 2004; Shenoy et al. 2007; Toth et al. 2007) (Fig. 1.5).

Sometimes, stress views are warranted for evaluation of ligamentous injuries. Examples include the clenched-fist view for assessment of scapholunate ligament integrity and the weight-bearing view for assessment of the coracoclavicular ligament. These views may demonstrate widening of the scapholunate interval and coracoclavicular distance, respectively, which indicate significant injury (Lee et al. 2011; Eschler et al. 2014). Without stress views, these injuries would likely be radiographically occult and hence be difficult to detect.

Fig. 1.2 An 87-year-old woman who presented with right ankle pain after a fall. (**a**) Frontal radiograph of the right ankle shows a spiral fracture of the distal tibia. (**b**) Frontal radiograph of the right leg shows a proximal fibular fracture (*arrow*). This Maisonneuve injury would have been missed if imaging coverage of the proximal leg was not performed

1.2.2 Radiographic Technique and Positioning

Radiographic technique refers to the selection of exposure factors, the kilovolt peak (kVp), and the milliampere-second (mAs), which determine the properties of the X-ray beam. The kVp influences the penetrative ability of the X-ray beam, while the mAs influences the quantity of radiation delivered. Good radiographic technique requires the proper selection of exposure factors such that there is optimal beam penetration of the anatomy, as well as optimal quantity of radiation reaching the detector at a radiation dose which is as low as reasonably achievable (ALARA).

In recent years, the field of diagnostic radiology has seen the transition from film/screen radiographic systems to digital imaging. For the film/screen systems, whether a film was under- or overexposed was easily appreciated, since the image would either be too white or too dark, respectively. In digital systems, however, the wide dynamic range of the detector and the ability to automatically post-process images to achieve optimal brightness allow images of acceptable quality to be produced over a larger range of exposures as compared to the film/screen systems (Murphey et al. 1992). Digital radiography is thus more forgiving with suboptimal exposures and has significantly reduced

Fig. 1.3 A 31-year-old woman who presented with left lateral ankle pain. Frontal and lateral radiographs of the left ankle were obtained. A minimally displaced distal fibular fracture is seen as a lucent line only on the lateral radiograph (*arrow*). It is occult on the frontal radiograph. This common injury illustrates the importance of having sufficient radiographic views for proper evaluation

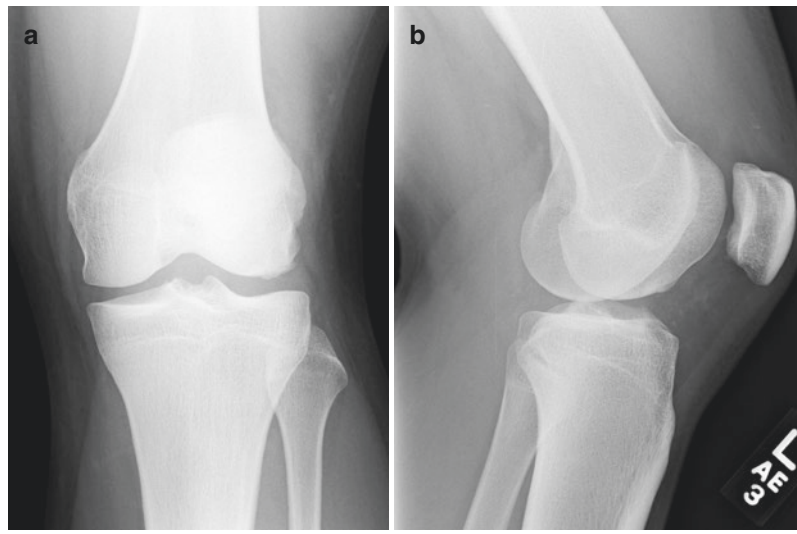

Fig. 1.4 An 18-year-old man who presented with left knee pain after a collision with another player during a football match. (**a**) Frontal and (**b**) lateral radiographs of the left knee show no fracture or dislocation. (**c**) Skyline view of the knee, however, shows a bony fragment at the medial aspect of the patella (*arrow*), suggestive of an avulsion fracture. (**d**) Axial fat-suppressed T2-W MR image of the left knee shows marrow edema at the site of the avulsion fracture (*arrow*) and disruption of the medial patellofemoral ligamentous structures (*arrowheads*), which are typical features of a transient patellar dislocation. Associated kissing bone contusion was present at the lateral femoral condyle (not shown)

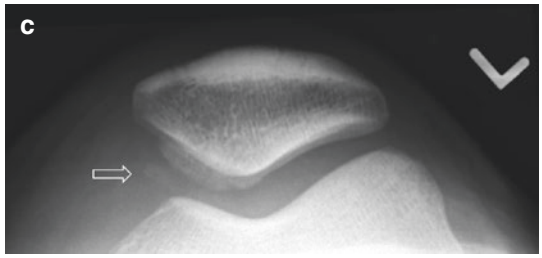

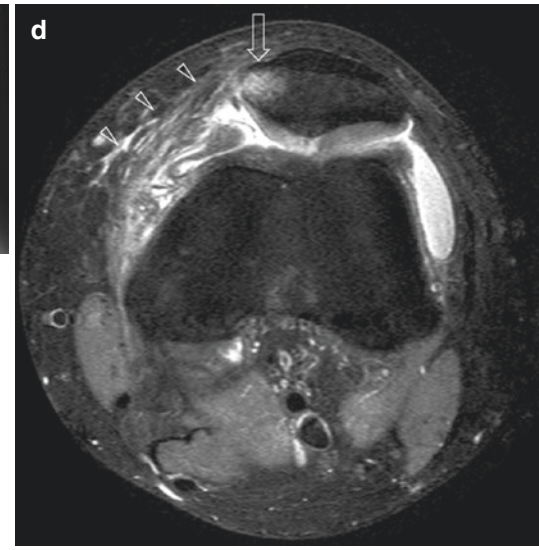

Fig. 1.4 (continued)

the number of rejected films. Even with the advantages of digital radiography, radiographic technique still affects the image quality and the radiation dose to the patient. Underexposure results in a reduction of the signal-to-noise ratio and manifests as increased quantum mottle, which might render the image unsuitable for diagnostic interpretation (Fig. 1.6). Conversely, overexposure in the digital system does not affect image quality but delivers a larger quantity of radiation than is necessary, resulting in excessive radiation dose to the patient. An optimum exposure should be given with each radiographic study, in line with the ALARA principle and producing an image of sufficient quality.

Each digital radiographic system is unique, due to differences in design and detector type. The optimal exposure settings are thus unique to each system. A technique chart should be available for each radiographic system, containing specific optimal exposure settings for each radiographic position in every region of the body. Exposure adjustment systems should then be applied to fine-tune the exposure settings based on the patient's weight and thickness of the body part to be imaged, the methods of which are beyond the scope of this chapter (Ching et al. 2014).

Standardized positioning of the patient results in radiographic views which are reproducible and optimal for interpretation. If proper positioning is not achieved during image acquisition, alignment of bones might not be accurately evaluated. For example, the posteroanterior view of the wrist should be obtained with the wrist in a neutral position, as only with proper positioning can the ulnar variance be accurately demonstrated. Supination of the forearm decreases ulnar variance, while pronation increases ulnar variance (Epner et al. 1982) (Fig. 1.7). Another example is in the radiographic evaluation of the ankle mortise. Accurate assessment of the alignment of the ankle mortise requires internal rotation of the leg and is not accurately assessed on standard anteroposterior views of the ankle (Takao et al. 2001).

Fig. 1.5 A 40-year-old man who presented with left wrist pain after falling onto his outstretched left hand. (**a**) Frontal and (**b**) lateral radiographs of the left wrist show no fracture or dislocation. (**c**) Posteroanterior view of the left wrist taken in ulnar deviation and slight tube angulation, usually part of the scaphoid imaging series, shows an undisplaced fracture of the waist of the scaphoid (*arrow*)

1.2.3 Radiographic Artifacts

Various technical artifacts can be produced during the acquisition and processing of radiographs (Shetty et al. 2011; Walz-Flannigan et al. 2012). Detailed discussion of this subject is beyond the scope of this chapter, but these artifacts are generally obvious and do not pose clinical diagnostic problems. Occasionally

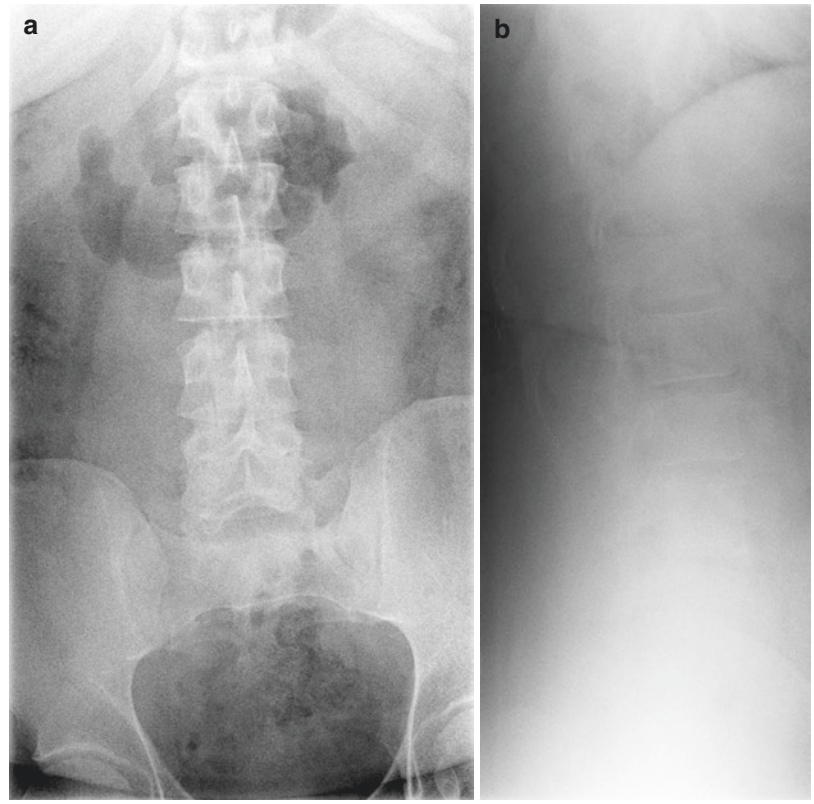

Fig. 1.6 A 29-year-old man who presented with low back pain following a motor vehicle accident. (**a**) Frontal and (**b**) lateral radiographs of the lumbar spine were obtained. Underexposure is evident, as a result of suboptimal radiographic technique. There is increase in quantum mottle especially on the lateral view, causing loss of radiographic detail and affecting the diagnostic quality of the study. This case illustrates how inappropriate selection of exposure factors can result in a poor-quality radiograph

though, with relevance to musculoskeletal imaging, technical artifacts secondary to dirt or dust may mimic foreign bodies. Encountering any of these technical artifacts would usually trigger a repeat of the radiographic examination. Nevertheless, a properly trained radiographer will be able to prevent many of these technical artifacts. Artifacts which are external to the patient may cause the underlying anatomical structures to be obscured. An external cast on a postreduction radiograph is a frequently encountered example. X-rays have difficulty penetrating the cast, resulting in reduced radiographic detail of the underlying bones (Fig. 1.8). Alignment of fractures and assessment of fracture healing can therefore be difficult to assess on these limited postreduction radiographs.

Fig. 1.7 Poor positioning affects the radiographic orthogonal views of the wrist in a 24-year-old man. (**a**) Posteroanterior and (**b**) lateral radiographs of the right wrist show inappropriate positioning of the wrist on the lateral view. After acquisition of the standard posteroanterior view, the wrist was left on the imaging plate with forearm supination performed for acquisition of the lateral view. Note the resultant identical appearances of the ulna on both images, making this a suboptimal radiographic study due to the lack of proper orthogonal views. (**c**) Posteroanterior and (**d**) lateral radiographs of the right wrist in another patient show appropriate positioning of the wrist, which remains in neutral position on both views. The ulnar variance is also influenced by the position of the wrist, increasing on pronation and decreasing on supination. Ulnar variance is therefore only accurately assessed on the standardized posteroanterior view of the wrist in the neutral position. It is noteworthy that dynamic stress maneuvers can also alter bony alignment. For example, the (**e**) frontal and (**f**) clenched-fist stress radiographs of the left wrist of a 40-year-old woman show an increase in ulnar variance on the stress view, which is a normal finding

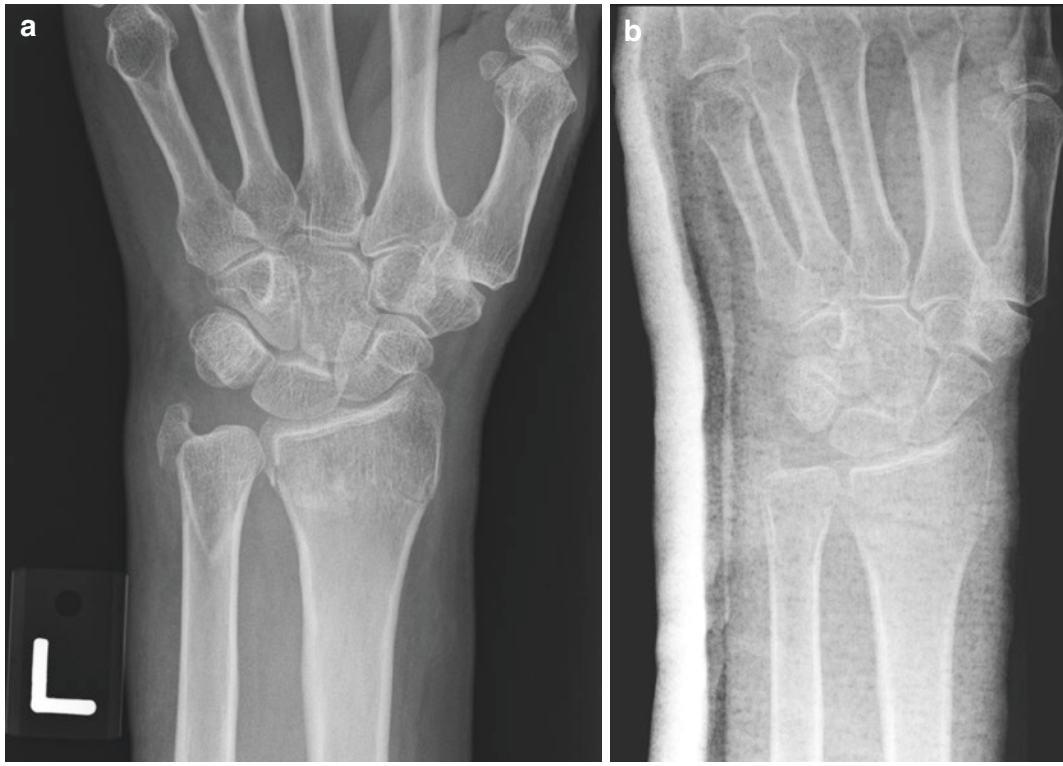

Fig. 1.8 A 66-year-old woman who presented after falling onto her outstretched left hand. (**a**) Frontal radiograph of the left wrist shows fractures of the distal radius and ulnar styloid process. (**b**) Postreduction frontal radiograph shows the presence of a backslab, which obscures the bony details

1.3 Limitations of Radiographic Imaging of Non-osseous Structures

One of the intrinsic limitations of radiography is its poor soft tissue contrast. Delineation of soft tissue structures on the radiograph may be difficult or impossible, making radiography a generally unreliable imaging modality for the assessment of soft tissue lesions. Unless there is gross morphological alteration (e.g., tendon rupture) (Fig. 1.9) or typical pattern of calcification or ossification (e.g., myositis ossificans) (Fig. 1.10), soft tissue abnormalities invariably go unnoticed on the radiograph. Radiography is generally an insensitive imaging modality compared to other cross-sectional imaging modalities, such as MRI and US imaging, in the early stages of disease processes involving the soft tissues. Early radiographic signs tend to be subtle and easily overlooked, whereas in advanced disease, osseous changes are usually readily observed. However, at the stage when such typically irreversible advanced osseous changes take place, the optimal time for therapeutic intervention might have been missed.

1.3.1 Intra- and Periarticular Structures

1.3.1.1 Articular Cartilage

The articular cartilage is essentially radiolucent and invisible on the radiograph. This makes its radiographic assessment particularly challenging. Radiographs are insensitive in the direct detection

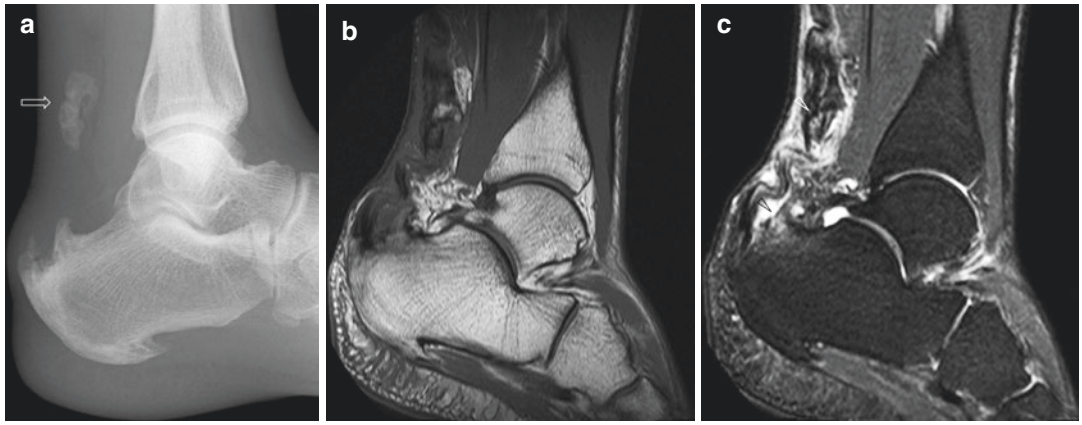

Fig. 1.9 A 41-year-old woman who presented after a fall with left ankle pain and had significant limited range of motion. (**a**) Lateral radiograph of the ankle shows background calcaneal enthesopathy, with an avulsed fragment off the dorsal aspect of the calcaneus (*arrow*). This finding, together with concordant clinical examination findings, allowed the diagnosis of a high-grade Achilles tendon tear to be made. (**b**) Sagittal T1-W MR image of the left ankle shows disruption of the fibers of the Achilles tendon in keeping with a complete tear. The associated avulsion fracture of the dorsal aspect of the calcaneus is seen, and on the (**c**) sagittal fat-suppressed T2-W MR image, there is corresponding marrow edema (*arrowheads*)

of chondral lesions, whether degenerative or traumatic in etiology. A purely chondral lesion caused by acute trauma, without involvement of the subchondral bone, cannot be appreciated on the radiograph (Fig. 1.11). The radiographic diagnosis of osteoarthritis is based on the observation of indirect features, such as the presence of marginal osteophytes, narrowing of joint space, as well as subchondral sclerosis and cyst formation. Radiographs have high specificity in the detection of advanced osteoarthritis, with the combination of indirect features allowing an easy diagnosis to be made. However, in early osteoarthritis, radiographs have low sensitivity and tend to underestimate the extent of cartilage degeneration (Blackburn et al. 1994). Despite the absence of radiographic signs of osteoarthritis, many symptomatic patients have been shown on arthroscopic evaluation to have significant degeneration of articular cartilage (Kijowski et al. 2006). In addition, the degree of joint space narrowing in patients with known osteoarthritis is a poor predictor of the actual state of the articular cartilage (Fife et al. 1991) (Fig. 1.12).

Currently, radiography is still widely used in the imaging follow-up of patients with established osteoarthritis. Nevertheless, with advances in pharmacological and surgical therapies, a more precise imaging modality is required for articular cartilage evaluation. MRI is currently the gold standard in the imaging evaluation of articular cartilage. It has the ability to assess both the morphology and the biochemical integrity of the articular cartilage and will play an increasingly important role in the noninvasive evaluation of articular cartilage both before and after therapeutic intervention (Gold et al. 2009; Crema et al. 2011).

1.3.1.2 Synovium and Joint Fluid

The synovium is normally not visible on the radiograph. When synovitis occurs, whether inflammatory such as in the inflammatory arthritides or infective in the case of septic arthritis, the radiographic appearance is usually normal early in the course of the disease. However, at this early stage, some changes may already be appreciated on MRI or US imaging. Synovial hypertrophy, hypervascularity and enhancement, and

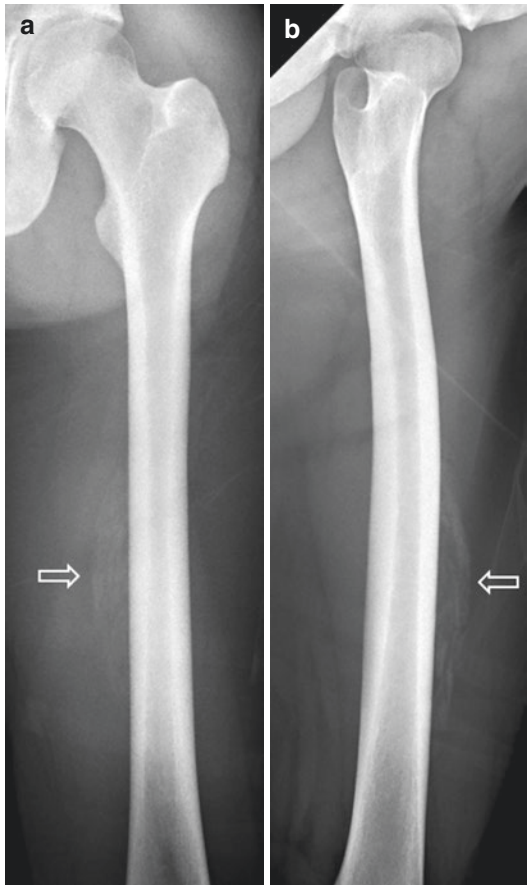

Fig. 1.10 A 17-year-old man who had a history of trauma to the left thigh 2 weeks before presentation. (**a**) Frontal and (**b**) lateral radiographs of the left femur show faint curvilinear sheet-like calcifications (*arrows*) adjacent to the mid-shaft of the femur. In the context of recent trauma, this appearance is highly suggestive of myositis ossificans. Note the external artifacts due to the patient's clothing

possible adjacent soft tissue and bone marrow signal changes are features which are usually radiographically occult (Fig. 1.13).

Small joint effusions may not be appreciated on radiography. Even if seen radiographically, without information on the state of the synovium, periarticular soft tissues, and bone marrow, this finding may not be useful in narrowing the differential diagnoses (Fig. 1.14). On the other hand, MRI, with or without intravenous contrast administration, is able to show the state of the surrounding structures, allowing better assessment of the underlying pathology. US imaging is highly sensitive in the detection of joint effusions and is able to provide real-time imaging guidance for diagnostic joint aspiration.

Radiographs have been used for more than a century in the imaging evaluation of the inflammatory arthritides, and they are able to demonstrate the osseous changes which indicate advanced disease. Currently, however, when modern therapy allows prevention or delay of irreversible joint destruction, imaging modalities with higher sensitivity for inflammatory changes (i.e., MRI and US imaging) are superior to radiographs in guiding treatment decisions (Szkudlarek et al. 2006; Weiner et al. 2008; Sankowski et al. 2013) (Fig. 1.15). Similarly, in the case of septic arthritis, irreversible joint destruction would have occurred by the time osseous changes are seen on the radiograph. Clinical judgment is of paramount importance in the management of patients with septic arthritis.

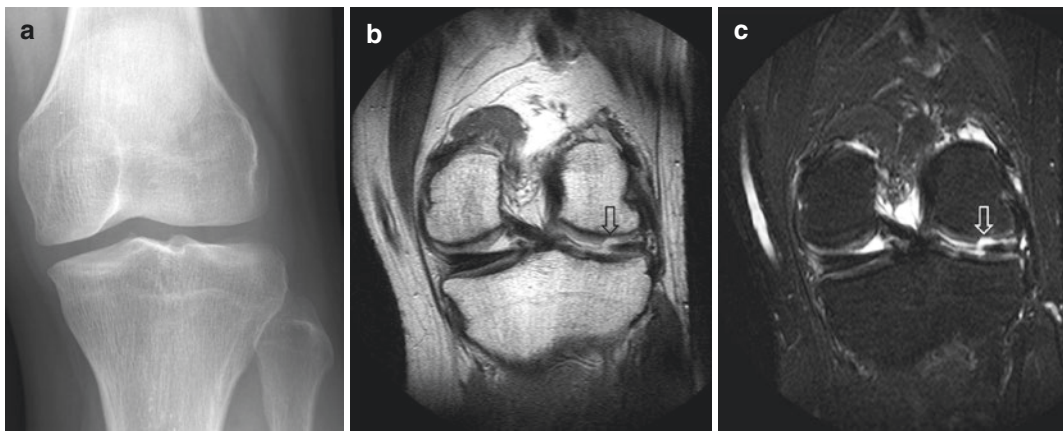

Fig. 1.11 A 42-year-old man who presented with left knee pain. (**a**) Frontal radiograph of the left knee shows minimal degenerative changes with preservation of the joint spaces. Coronal (**b**) PD-W and (**c**) fat-suppressed T2-W MR images of the left knee show a focal chondral defect (*arrows*) at the articular surface of the lateral femoral condyle. This finding cannot be appreciated radiographically since cartilage is essentially radiolucent

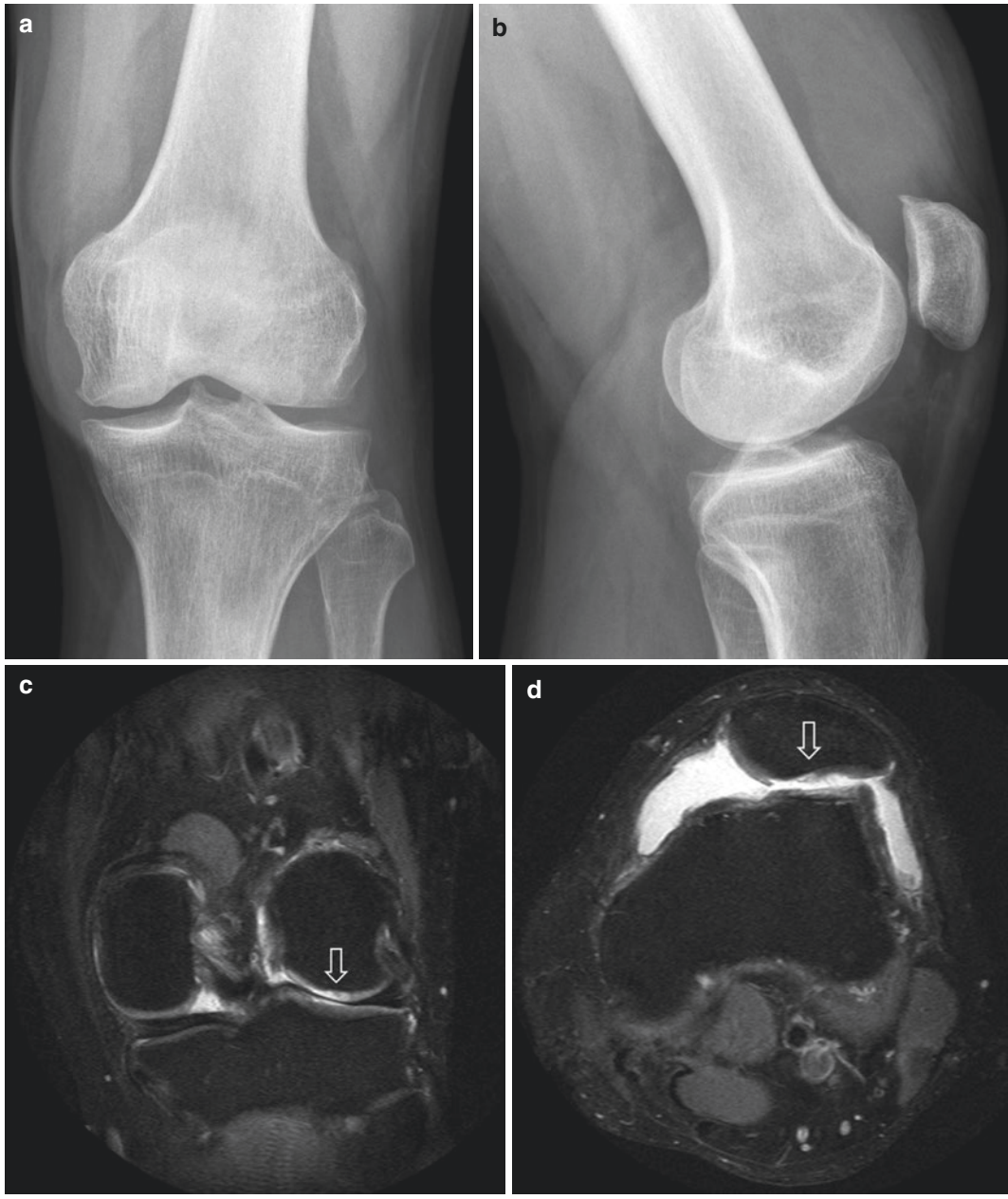

Fig. 1.12 A 44-year-old man who presented with chronic left knee pain. (**a**) Frontal and (**b**) lateral radiographs of the left knee show mild osteoarthritis with small marginal osteophytes and relative preservation of the joint spaces. A joint effusion is also noted. (**c**) Coronal and (**d**) axial fat-suppressed PD-W MR images of the left knee show partial- to full-thickness articular cartilage loss (*arrows*) involving the lateral tibiofemoral and patellofemoral joint compartments and confirm the presence of a joint effusion. As illustrated, the degree of joint space narrowing is not a sensitive method for predicting the actual state of the articular cartilage

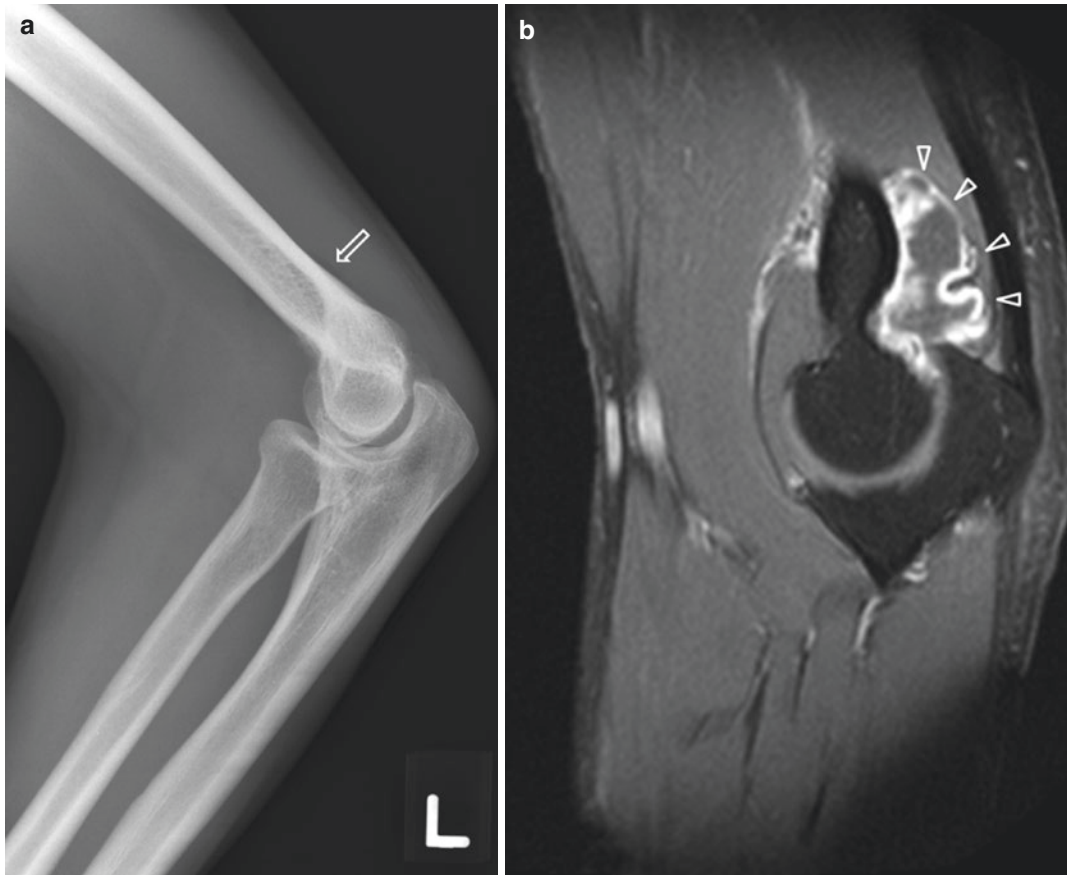

Fig. 1.13 A 36-year-old man who presented with left elbow pain after a traumatic injury. Initial radiographic evaluation of the left elbow was negative for fracture or dislocation. (**a**) Lateral radiograph shows that the posterior fat pad is just visible (*arrow*), raising suspicion of a joint effusion. (**b**) Sagittal contrast-enhanced fat-suppressed T1-W MR image of the left elbow confirms the presence of a joint effusion and shows enhancement of the synovium (*arrowheads*), consistent with synovitis. No fracture was identified. In the absence of other clinical features of infection, transient inflammatory synovitis of traumatic etiology was the primary diagnosis. The patient made a full recovery with conservative management

Joint aspiration has to be performed for the diagnosis to be established, and treatment has to be instituted without delay, as rapid progression to permanent joint destruction may otherwise ensue.

1.3.1.3 Ligaments, Tendons, and Other Fibrocartilaginous Structures

Radiographic assessment of ligaments, tendons, and fibrocartilaginous structures relies upon the observation of indirect features which indicate possible underlying pathology involving these structures. These indirect features include joint malalignment, hemarthrosis, calcific deposits, and secondary osseous changes. The latter two are seen in relation to chronic degenerative processes. In acute trauma, injuries to these structures tend to be occult on the radiograph, especially when sprains, strains, or partial tears occur. Extensive ligamentous disruption with joint dislocation is usually visible

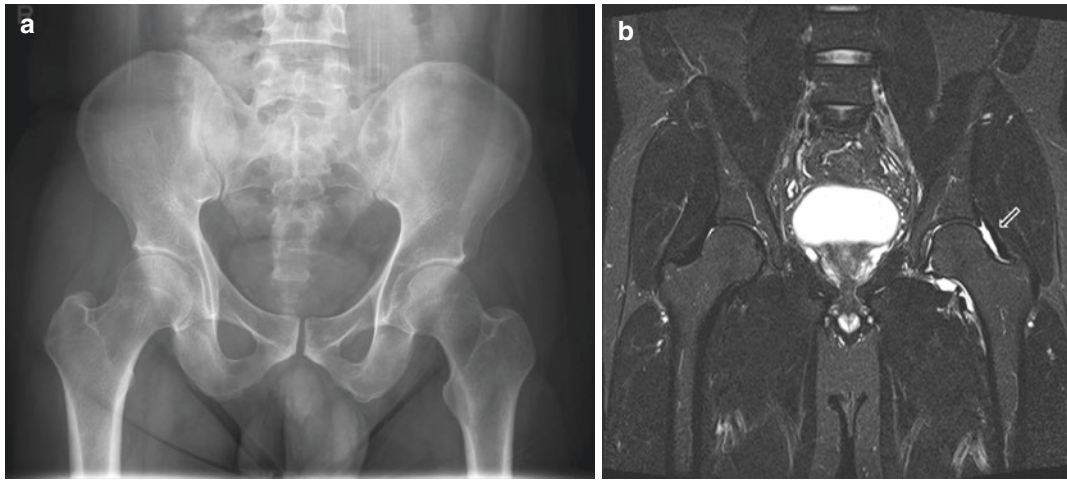

Fig. 1.14 A 38-year-old man who presented with left groin pain after a period of intense physical activity. (**a**) Frontal radiograph of the pelvis is essentially normal. (**b**) Coronal turbo inversion recovery magnitude (TIRM) MR image of the pelvis shows a left hip joint effusion (*arrow*), which was radiographically occult. This represented a reactive effusion secondary to a left groin muscular strain (not shown), and the patient subsequently made a full recovery with conservative management

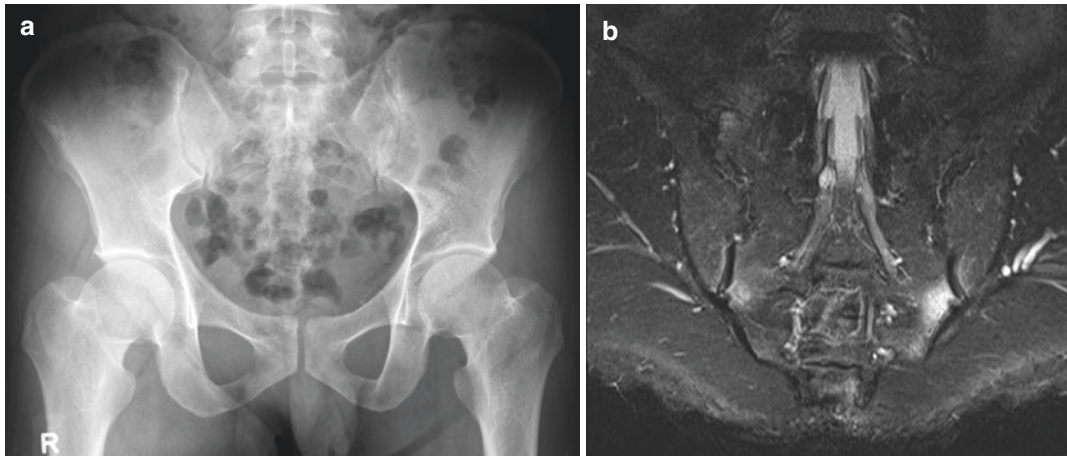

Fig. 1.15 A 35-year-old man who presented with worsening back pain, on a background of chronic back and polyarticular pain. (**a**) Frontal radiograph of the pelvis shows no significant abnormality. (**b**) Coronal TIRM MR image of the sacrum shows periarticular marrow edema involving the inferior aspect of both sacroiliac joints (worse on the left), seen as conspicuous hyperintense fluid signal which has high contrast compared with the surrounding fat-suppressed normal marrow. This case highlights the high sensitivity of MRI to the early changes of sacroiliitis, when it is radiographically occult

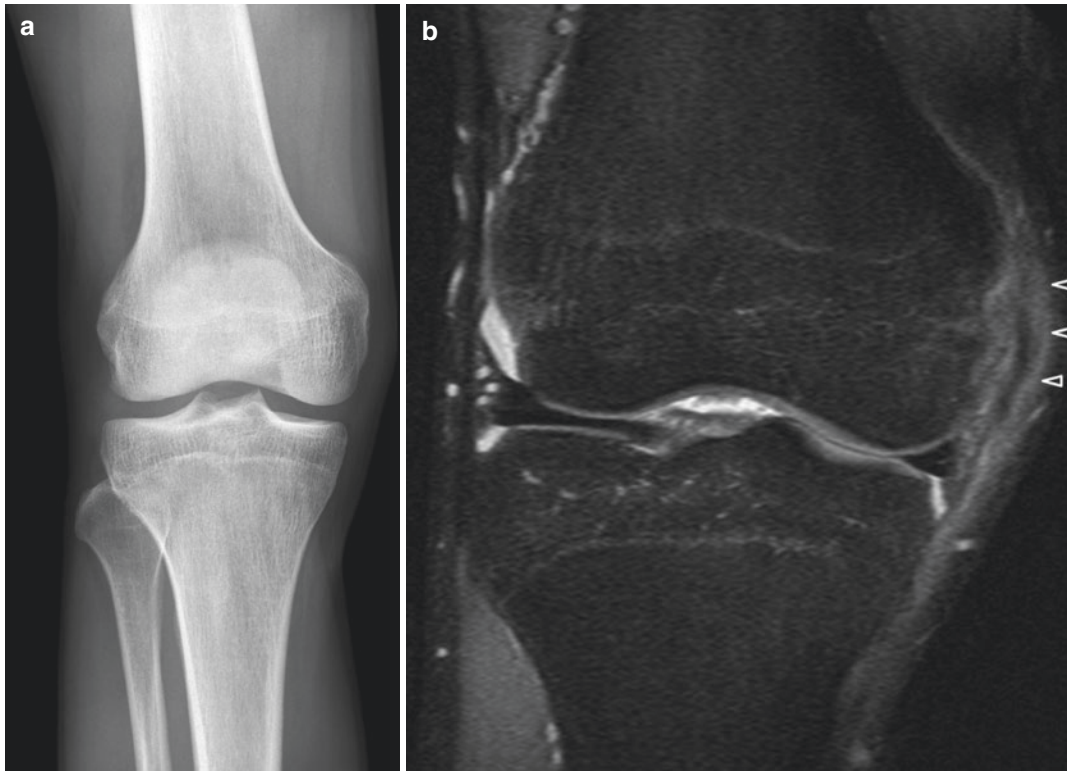

Fig. 1.16 A 25-year-old man who presented with right knee pain after sustaining an injury from a tackle during a football match. (**a**) Frontal radiograph of the right knee shows no fracture or dislocation. (**b**) Coronal fat-suppressed PD-W MR image of the right knee shows a grade 2 injury of the medial collateral ligament, evident as a partial disruption of the ligament with surrounding edema (*arrowheads*). This injury is usually not appreciable on radiography, but may be suggested if bony avulsion occurs at the attachment sites of the ligament

on the radiograph. Complete tendon rupture with tendon retraction may also be visible radiographically. However, these injuries tend to be obvious on clinical examination.

Gross disruption of the supporting ligaments of a joint, with the presence of dislocation, represents one end of the spectrum of ligamentous injuries and manifests in radiographs as a disruption of the bony alignment. Less severe ligamentous injuries range from sprains to high-grade partial tears and even complete tears of individual ligaments. These injuries are largely not appreciated on radiographs, especially in the acute setting when joint instability might not be accurately assessed on clinical examination, and the bony alignment often remains normal on imaging (Figs. 1.16 and 1.17). Sometimes, the same traumatic mechanism causing ligamentous injury may result in bone abnormalities, which again are indirect features on the radiograph. These bone abnormalities can often be seen on the radiograph but are usually subtle and easily missed, if not suspected. In the example of an injury involving the anterior cruciate ligament of the knee, possible bony abnormalities include avulsion fractures at the femoral or tibial attachment sites, the Segond fracture, and an osteochondral impaction fracture of the lateral femoral condyle (Ng et al. 2011). Detection of any of these bony abnormalities without appreciating the underlying soft tissue injuries is a potential pitfall in the interpretation of the radiograph.

A complete tendon rupture with tendon retraction, involving a superficial large tendon such as the Achilles tendon, does not usually pose a diagnostic problem. However, in other locations, for example, the rotator cuff tendons in the shoulder, accurate assessment of tendon

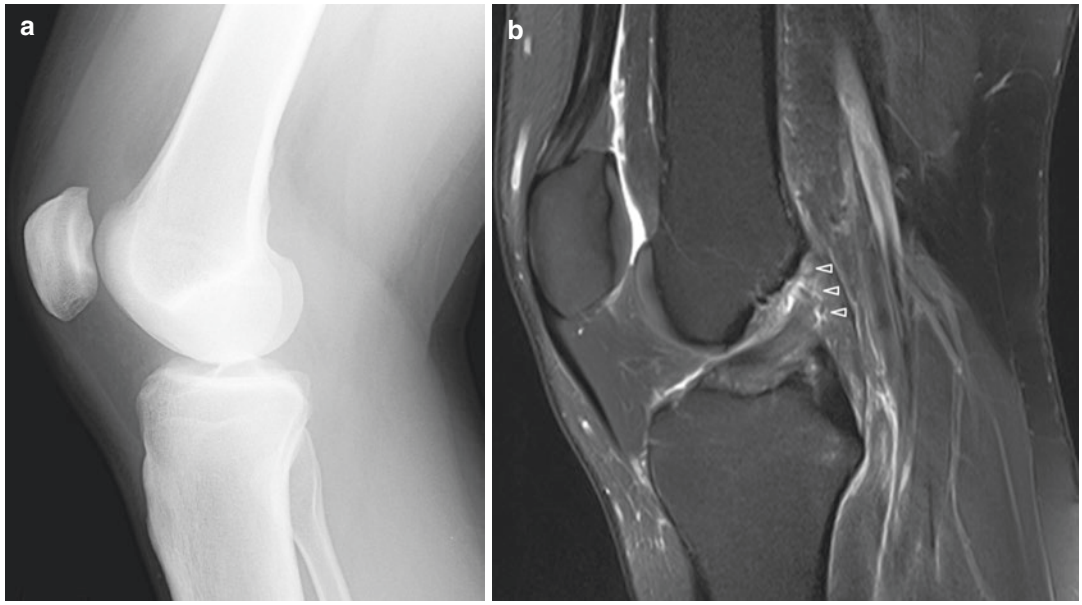

Fig. 1.17 A 35-year-old man who presented with right knee pain after a twisting injury sustained during a game of basketball. (**a**) Lateral radiograph of the right knee shows no significant bony injury or joint malalignment. A small suprapatellar joint effusion is noted. (**b**) Sagittal fat-suppressed PD-W MR image of the right knee shows a high-grade injury of the anterior cruciate ligament, evident as a disruption of the fibers at the femoral attachment (*arrowheads*). This injury is not usually discernable on radiography, although indirect osseous findings (such as Segond fracture) may suggest this injury

tears is impossible on radiographs. The rotator cuff is the archetype of a tendon which is highly susceptible to chronic degeneration. Significant chronic tendinosis and tendon tears of the rotator cuff are typically not visualized on radiographs (Fig. 1.18), though indirect findings such as osseous changes (signifying advanced disease), calcific tendinous deposits, and features of subacromial impingement may be seen. Nevertheless, other imaging modalities such as MRI and US imaging would be necessary for proper evaluation, as radiographic findings alone will not be sufficient to guide clinical management (Seibold et al. 1999). Other examples of fibrocartilaginous structures which are usually not directly visualized on radiography include intervertebral disks, menisci of the knee, glenoid labrum, and triangular fibrocartilage complex of the wrist (Figs. 1.19, 1.20, 1.21, and 1.22). Radiography plays a limited but usually complementary role in the evaluation of these structures.

1.3.2 Other Soft Tissues and Foreign Bodies

Various soft tissues, such as muscle and subcutaneous soft tissue, are usually included in the views obtained on radiography of the musculoskeletal system. Radiographs are largely limited in the assessment of muscle abnormalities, with rare exceptions such as myositis ossificans which shows typical radiographic appearances but may be diagnostically confusing on MRI early in its course (McCarthy and Sundaram 2005). Otherwise, muscle lesions are best assessed on MRI, which can demonstrate alterations in muscle signal intensity characteristics (Theodorou et al. 2012).

However, much information can still be gleaned from the radiographic appearance of the subcutaneous soft tissue. Diffuse processes such as edema and cellulitis may be appreciated by the presence of increased reticular markings and thickening of the overlying skin. However, this appearance is nonspecific, based on radiography

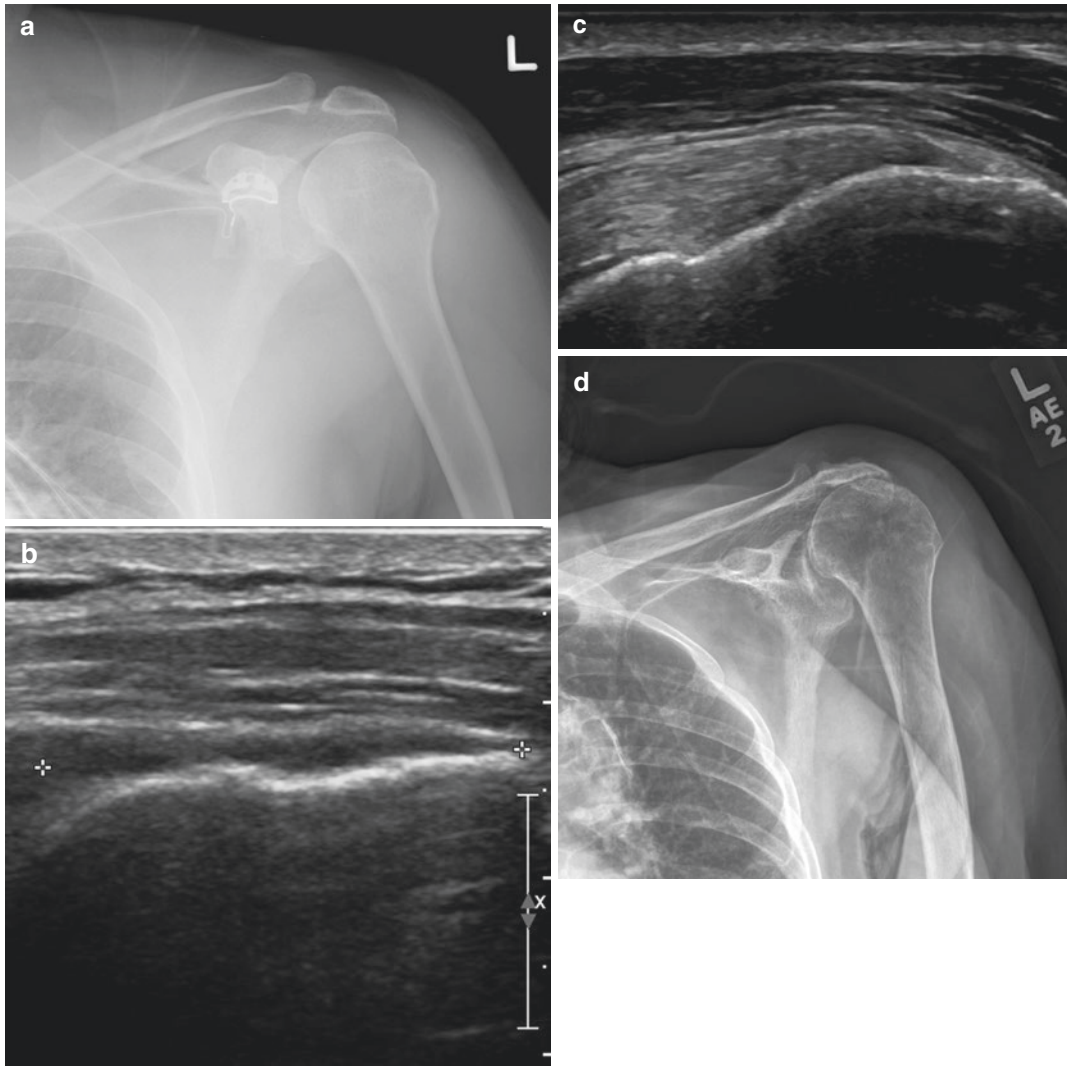

Fig. 1.18 A 46-year-old man who presented with left shoulder pain and decreased range of motion after a motor vehicle accident. (**a**) Frontal radiograph of the left shoulder shows no significant abnormality. The humerus is in an internally rotated position. (**b**) Longitudinal US image of the supraspinatus shows a complete tear of the supraspinatus tendon, with a tendon gap at its attachment to the greater tuberosity (as indicated by the crosshairs). This finding was not apparent on the radiographs. (**c**) Longitudinal US image of another patient shows a normal fibrillar pattern of the distal supraspinatus tendon (shown for comparison). (**d**) Frontal radiograph of the left shoulder of a 70-year-old woman with advanced rotator cuff disease shows an obliterated acromiohumeral interval and secondary degenerative osseous changes, features which are radiographically discernible. At this late stage of disease, surgical intervention will not be useful

alone. Likewise, for focal pathologies such as superficial hematoma, abscess, and a myriad of other soft tissue masses (including intramuscular masses), the radiographic appearance alone is usually nonspecific. Certain radiographic characteristics such as lesion density, the presence of calcification or ossification, and effect on adjacent osseous structures may shed some light on the nature of the soft tissue mass. Thus, although limited on its own, radiography plays a

Fig. 1.19 A 25-year-old woman who presented with low back pain and bilateral lower limb numbness after lifting some heavy loads. (**a**) Lateral radiograph of the lumbar spine is essentially normal. (**b**) Sagittal fat-suppressed T2-W MR image of the lumbar spine shows posterior intervertebral disk extrusions at L4–L5 and L5-S1 levels (*arrows*), worse at the L4–L5 level where there is significant spinal canal stenosis with likely impingement of the cauda equina nerve roots. Note the reduced signal of the desiccated disks at the affected levels, as well as increased marrow signal at the endplates of L4–L5 level consistent with Modic type 1 degenerative signal changes. The other intervertebral disks have a normal appearance. Example of fibrocartilaginous structure (disk) not directly visualized on radiography

complementary role in the imaging evaluation of soft tissue masses (Gartner et al. 2009).

Radiographs are useful for the detection of suspected radiopaque foreign bodies, as well as soft tissue gas pockets. On the radiograph, gas pockets are visible on a background of soft tissue densities as their hyperlucency provides imaging contrast. Similarly, radiopaque foreign bodies can be seen, as the differences in densities provide good contrast. The higher the radiodensity of a foreign body, the greater its visibility. A limitation of radiography is in the detection of foreign bodies which are weakly radiopaque, especially if the material of the foreign body has a density close to that of the surrounding soft tissue (e.g., wood). These weakly radiopaque foreign bodies will not be appreciated on the radiograph. This potential pitfall should be recognized by the clinician requesting the radiograph, and if necessary, an alternative imaging modality such as US imaging should be considered (Aras et al. 2010) (Fig. 1.23).

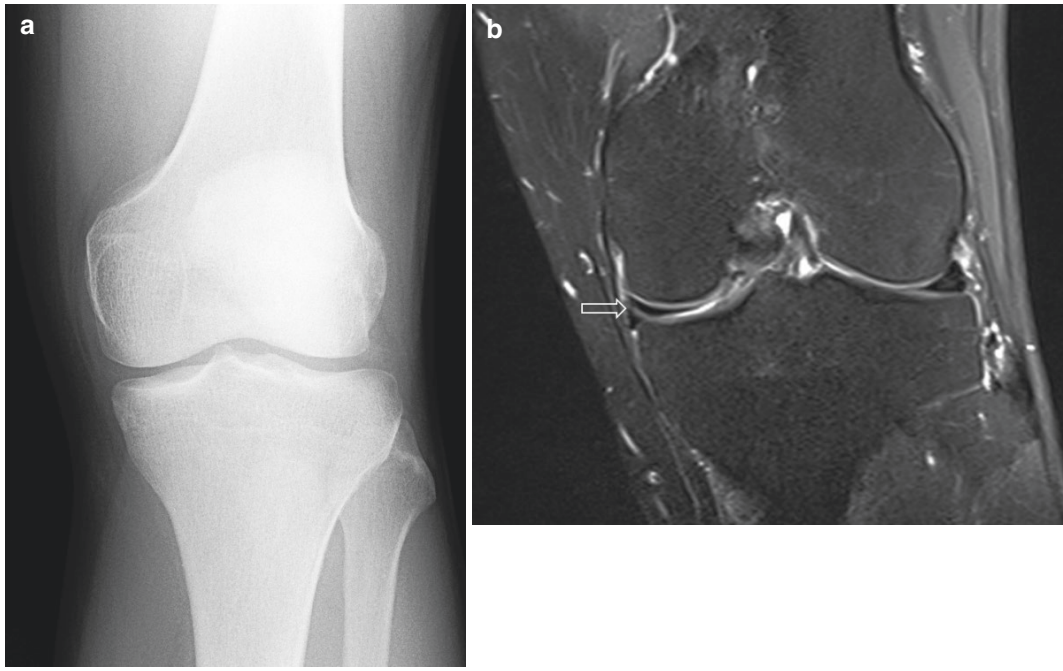

Fig. 1.20 A 37-year-old man who presented with left knee pain. (**a**) Frontal radiograph of the left knee shows no significant abnormality. (**b**) Coronal fat-suppressed PD-W MR image of the left knee shows a horizontal tear of the medial meniscus involving its inferior surface, evident as a linear area of hyperintensity (*arrow*). The lateral meniscus has a normal appearance. Example of fibrocartilaginous structure (meniscus) not directly visualized on radiography

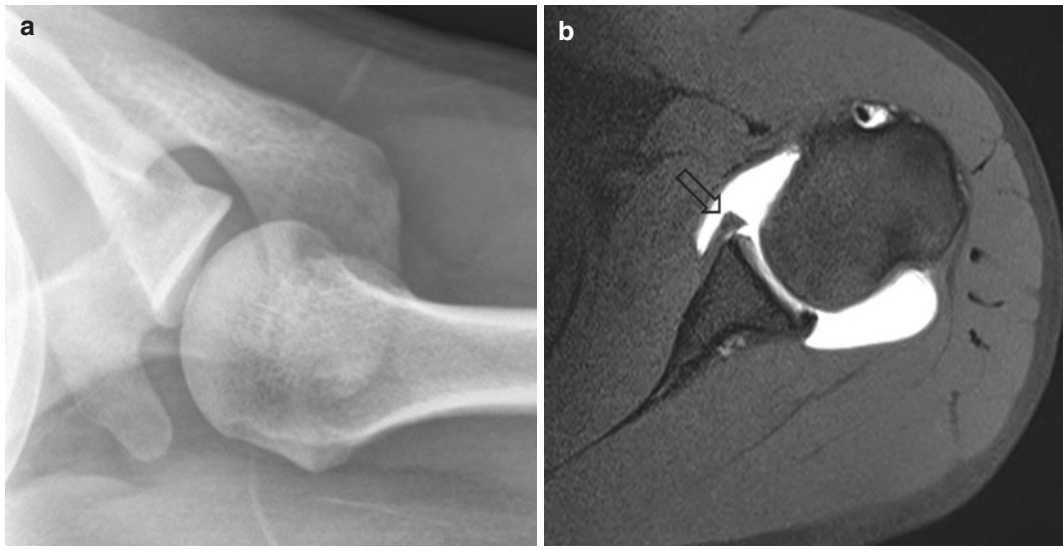

Fig. 1.21 A 22-year-old man who had recurrent episodes of anterior shoulder dislocation. (**a**) Axillary radiographic view of the left shoulder shows normal joint alignment and no significant osseous abnormality. (**b**) Axial fat-suppressed T1-W MR arthrographic image of the left shoulder shows a Perthes lesion (a variant of the Bankart lesion), manifesting as detachment of the anteroinferior glenoid labrum which remains attached to an intact but lifted periosteum of the anterior glenoid (*arrow*). The posterior glenoid labrum shows a normal appearance. Example of fibrocartilaginous structure (glenoid labrum) not directly visualized on radiography

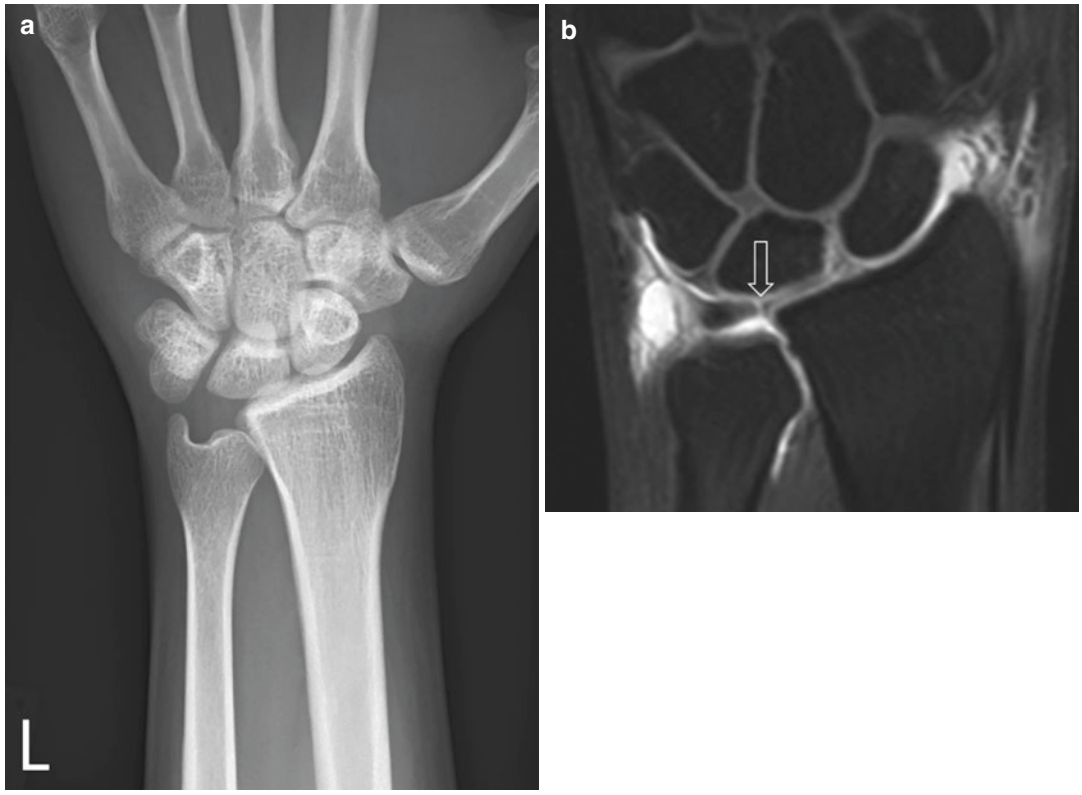

Fig. 1.22 A 28-year-old motorcyclist who had persistent ulnar-sided left wrist pain 4 months after being involved in a minor motor vehicle accident. (**a**) Frontal radiograph of his left wrist is essentially normal, with no fracture or dislocation seen. Negative ulnar variance is noted. (**b**) Coronal fat-suppressed T1-W MR arthrographic image of the left wrist shows a tear of the radial attachment site of the triangular fibrocartilage complex (TFCC), seen as linear high signal (*arrow*). Hyperintense contrast agent is seen extending into the distal radioulnar joint, a result of the TFCC tear. Example of fibrocartilaginous structure (TFCC) not directly visualized on radiography

Fig. 1.23 A 34-year-old construction worker who presented with pain in the right foot after stepping barefoot onto unknown material at his work site. (**a**) Lateral radiograph of the right foot does not show any radiopaque foreign body. (**b**) US image shows a few small foreign bodies within the plantar subcutaneous layer of the right foot, seen as linear echogenic structures (as indicated by the *crosshairs*). The patient underwent removal of the foreign bodies, which turned out to be wooden splinters. Wood is weakly radiopaque and may be invisible on radiography

1.4 Radiographically Occult Osseous Abnormalities

One of the strengths of the radiograph is its ability to demonstrate the osseous structures. This gives it relatively good specificity in the evaluation of osseous abnormalities. In most cases of discrete osseous lesions, the radiographic appearance allows categorization into aggressive and nonaggressive entities and so helps narrow the differential diagnoses. In many cases, the radiographic appearance is so characteristic as to allow a diagnosis to be made.

1.4.1 Destructive Osseous Lesions

Although radiographs display osseous anatomy well, before a destructive osseous lesion is even

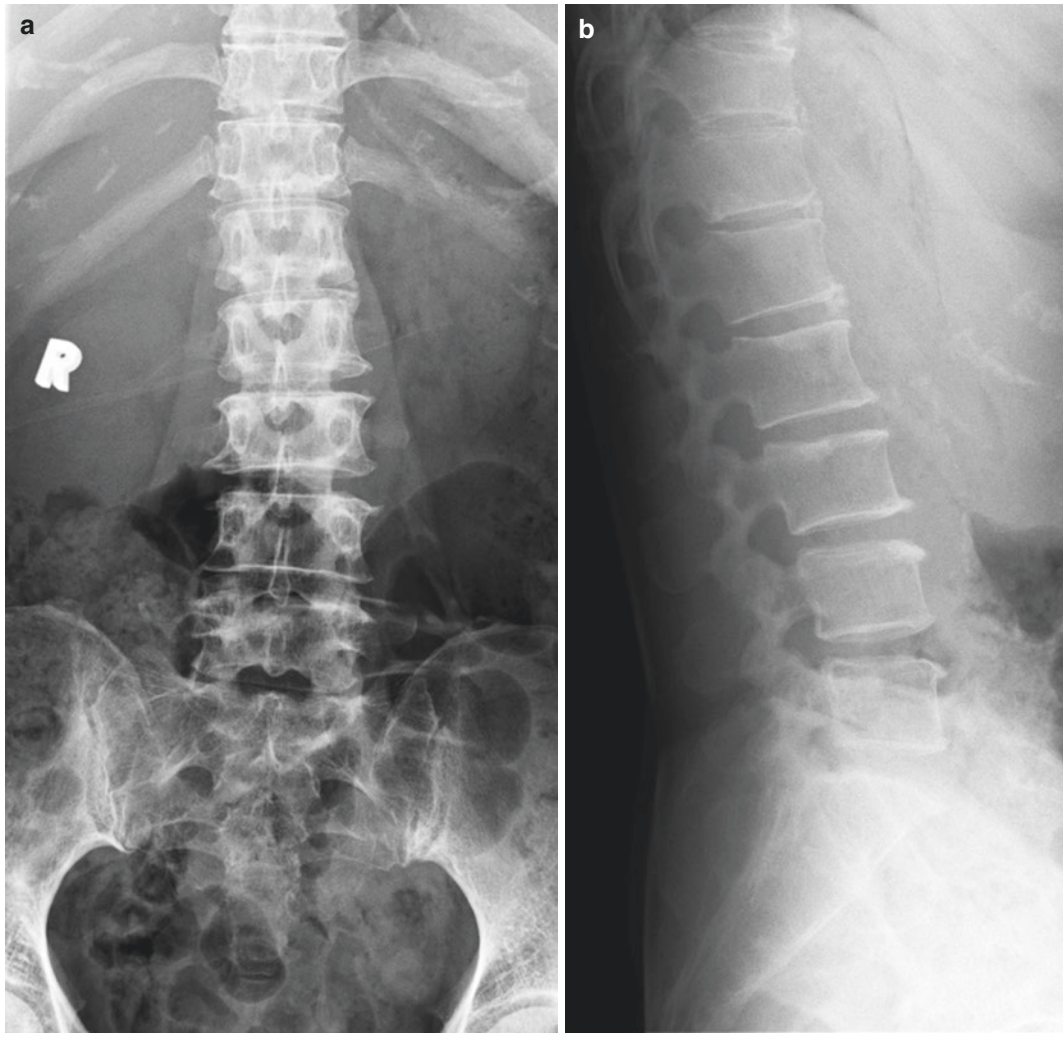

Fig. 1.24 A 53-year-old woman who was recently diagnosed with adenocarcinoma of the right lung and presented with diffuse back pain. (**a**) Frontal and (**b**) lateral radiographs of the lumbar spine show spondylotic changes. Bone density is preserved and there is no evidence of osseous destruction. (**c**) Whole-body Tc-99 m MDP bone scintiscan shows extensive osseous metastases, evident as increased tracer uptake at multiple sites, especially in the axial skeleton including the lumbar spine. This case demonstrates the superior sensitivity of bone scintigraphy compared to radiographs in the detection of metastatic bone disease

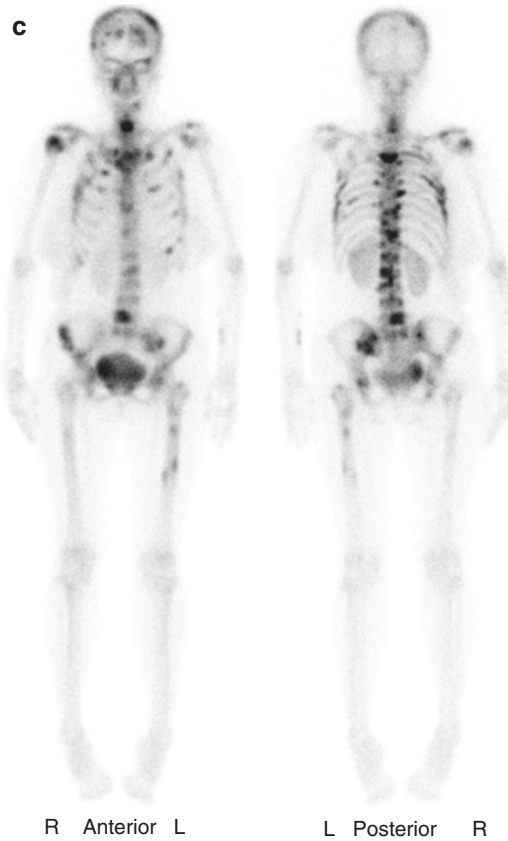

Fig. 1.24 (continued)

visible radiographically, there has to be loss of about 50% of the cortical bone mass (Osmond et al. 1975; Taoka et al. 2001). Radiography is thus significantly limited in the detection of lesions early in the course of osseous metastatic disease, since the pathology is predominantly confined to the medullary cavity of the bone at this early stage (Gold et al. 1990). In contrast to radiography, bone scintigraphy is sensitive enough to demonstrate metastatic involvement of cortical bone with a threshold of about 5–10% lesion-to-normal bone ratio (Algra et al. 1991) (Fig. 1.24).

Similarly, in osteomyelitis, before thresholds of about 50% of bone mineral content involvement and 1 cm of lesion size are reached, the lesion remains radiographically occult (Pineda et al. 2009). Thus, the radiographic features of osteomyelitis are typically delayed by about 10–14 days from the onset of infection. In the early stages of osteomyelitis, the radiograph can be normal in appearance and so is significantly limited as a diagnostic modality. However, radiographs can still be useful for demonstrating associated findings such as foreign bodies and soft tissue gas in this setting. MRI is exquisitely sensitive to bone marrow changes, making it the imaging modality of choice in the evaluation of vertebral metastases as well as osteomyelitis, both of which mainly involve the bone marrow (Algra et al. 1991; Pineda et al. 2009) (Figs. 1.25 and 1.26).

1.4.2 Trauma-Related Osseous Injuries

1.4.2.1 Undisplaced Fractures

An important limitation of radiographs is in the evaluation of acute undisplaced fractures, especially hairline ones. For an acute fracture to be visualized on the radiograph, at least a small amount of displacement or separation is usually necessary for the fracture to manifest as a radiolucent line, sclerotic line, or cortical step. Hence, even with adequate views and proper technique, an acute undisplaced fracture can be radiographically occult. It is important to be aware of this potential pitfall when interpreting radiographs of the acute trauma patient, especially if there are associated soft tissue findings in a seemingly negative radiograph. For example, elevated fat pads in the elbow joint indicate the presence of a hemarthrosis, which could be secondary to an occult undisplaced fracture. If the clinical suspicion for a fracture is high despite a negative initial radiograph, follow-up radiographs can be obtained 10–14 days later. If present, these fractures typically become increasingly visible with time as bone resorption and callus formation occur at the fracture site (Fig. 1.27).

In certain clinical scenarios, confirmation of the presence of a fracture may need to be done rapidly, as an unnecessary delay in the diagnosis would result in significant morbidity. In such cases, follow-up radiographs should not be advocated and advanced imaging evaluation should instead be performed. For example, in the elderly

Fig. 1.25 A 62-year-old man with type 2 diabetes mellitus who presented with an infected ulcer at the left hindfoot. (**a**) Lateral radiograph of the left ankle shows a radiolucent area posterior to the calcaneum (*arrow*), corresponding to the known ulcer. No obvious radiographic sign of osteomyelitis (e.g., periosteal reaction and bone destruction) is discerned. (**b**) Sagittal TIRM MR image of the left foot shows subcutaneous inflammatory signal alteration deep to the ulcer (*arrowheads*), extending down to the calcaneum which shows abnormal marrow edema (*asterisk*). (**c**) Sagittal T1-W MR image shows the characteristic T1-hypointense marrow signal of osteomyelitis involving the calcaneum (*asterisk*)

adult with hip pain after a fall, where there is inability to weight-bear and no fracture is seen on radiographs, further advanced imaging such as MRI and CT should be arranged early to establish the presence of an undisplaced femoral neck fracture, which usually requires to be treated surgically (Oka and Monu 2004; Gill et al. 2013; Ward et al. 2013) (Fig. 1.28).

1.4.2.2 Stress Injuries

Stress injuries range in a continuum from stress reactions to established stress fractures. They develop as a result of chronic repetitive microtrauma causing fatigue of normal bone and essentially comprise microtrabecular fractures which are not visible on the radiograph. If the inciting activity causing repetitive stress is not stopped to allow bone to heal, these microtrabecular fractures accumulate and eventually result in a full cortical fracture. Formation of periosteal new bone is the earliest radiographic feature of stress fractures, and its appearance may be delayed up to 3 months from the initial injurious stimulus (Jarraya et al. 2013) (Fig. 1.29).

The earliest stage of stress injuries, termed stress reaction, is radiographically occult but may manifest on MRI as bone marrow edema without a fracture line. Due to nonspecificity of isolated bone marrow edema, CT may also be useful in distinguishing stress reaction from other entities such as osteoid osteoma (Liong and Whitehouse 2012). Since only timely management can interrupt the cycle of repetitive stress, early detection of stress injuries is crucial. An understanding of the limitation of radiography in this respect and the use of more appropriate imaging modalities is vital in establishing the diagnosis of stress injury in the early stages.

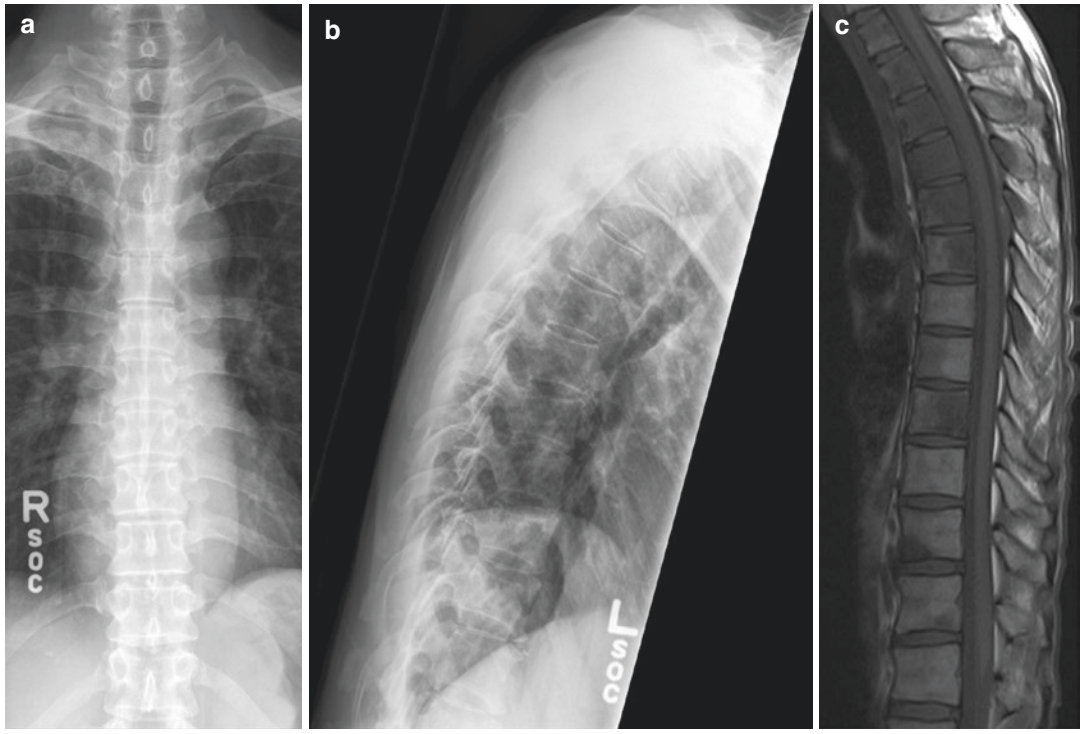

Fig. 1.26 A 51-year-old man who presented with back pain of insidious onset. (**a**) Frontal and (**b**) lateral radiographs of the thoracic spine appear essentially normal. There is no radiographic evidence of osseous metastasis. (**c**) Sagittal T1-W MR image of the thoracic spine shows abnormal hypointense marrow signal involving multiple vertebral levels. The patient had extensive osseous metastases secondary to a primary malignancy in the right lung apex, which was incidentally imaged on the frontal radiograph (**a**) and seen as right lung apical opacities

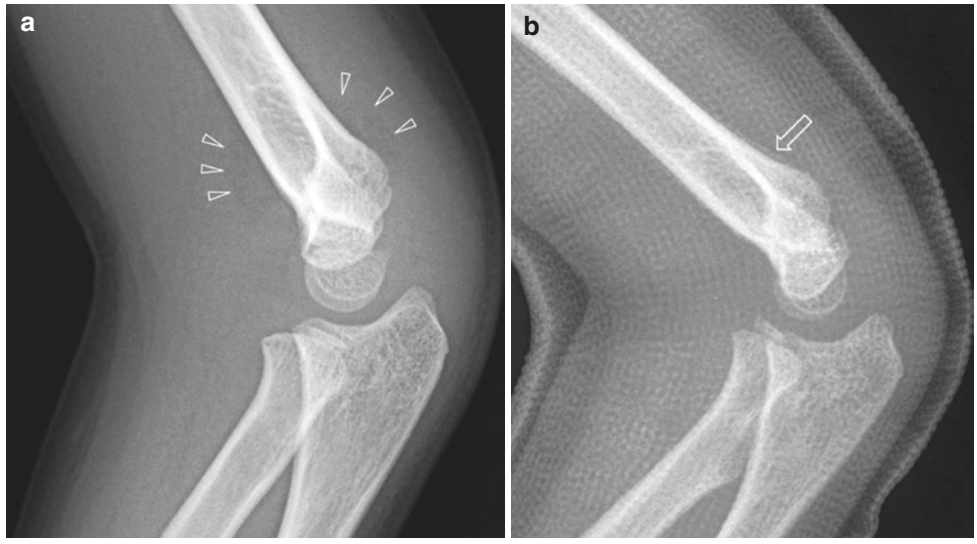

Fig. 1.27 A 6-year-old boy who presented with pain in the left elbow after a fall onto his outstretched left hand. (**a**) Lateral radiograph of the left elbow shows no displaced fracture. The joint alignment is maintained. There is however a joint effusion, as indicated by elevated anterior and posterior fat pads (*arrowheads*). This finding should raise the suspicion of an occult undisplaced fracture in the setting of trauma. (**b**) Follow-up lateral radiograph of the left elbow was performed 10 days after the initial presentation. Despite the presence of an overlying cast, periosteal reaction can be seen along the posterior aspect of the distal shaft of the humerus (*arrow*), indicating a healing undisplaced fracture

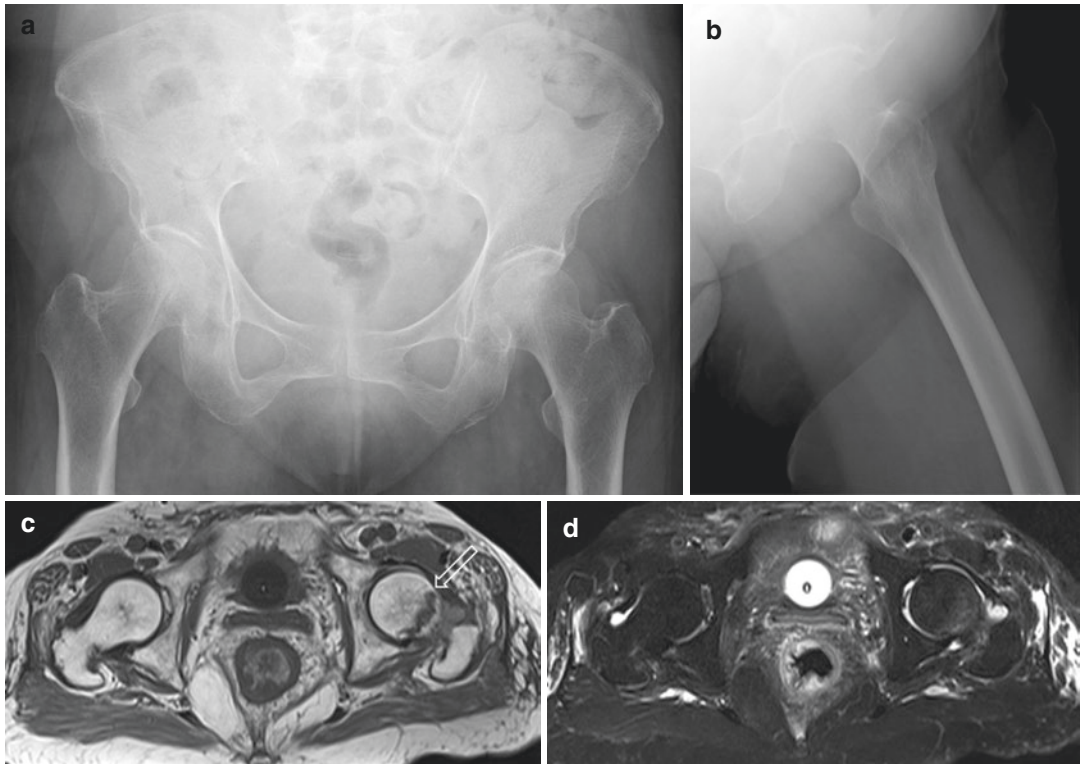

Fig. 1.28 An 83-year-old woman who presented with left hip pain after a fall. (**a**) Frontal radiograph of the pelvis and (**b**) lateral radiograph of the left hip show no appreciable fracture or dislocation. There is diffuse reduction in bone density, which limits radiographic sensitivity for minimally displaced fractures. (**c**) Axial T1-W MR image of the pelvis shows an undisplaced fracture of the neck of the left femur, seen as a hypointense fracture line (*arrow*). This fracture was radiographically occult. (**d**) Axial fat-suppressed T2-W MR image of the pelvis at the corresponding level shows associated marrow edema around the fracture site

1.4.3 Osteoporosis

Osteoporosis is defined as a reduction in bone mass, with a bone density of less than 2.5 standard deviations below that of a healthy young adult (World Health Organization 2003). It has many different causes, but its appearance on radiography is the same regardless of etiology. The diagnosis is most confidently made on a quantitative technique such as dual-energy X-ray absorptiometry (DXA). However, most cases of osteoporosis are still diagnosed on radiography (Guglielmi et al. 2011). Radiographs are inherently limited in the detection of reduced bone mass, which is only appreciable when about 30% of bone loss has occurred (Harris and Heaney 1969). Radiographic technique may also be a confounding factor, for example, causing bones to appear more radiolucent than usual and giving a false impression of osteoporosis. This is a potential pitfall when radiographs are used in the diagnosis of osteoporosis. A combination of features such as cortical thinning, trabecular changes, and insufficiency fractures is usually needed to provide a higher degree of confidence in the diagnosis of osteoporosis on radiography (Fan and Peh 2016). Another radiographic pitfall in relation to osteoporosis is the limitation in the detection of destructive lesions and fractures. On a background of reduced bone mass, these conditions can be difficult or impossible to

Fig. 1.29 A 24-year-old avid runner who presented with right foot pain. (**a**) Frontal and (**b**) oblique radiographs of the right foot show no significant abnormality. Incidental note is made of a type 2 os navicularis. (**c**) Sagittal T1-W MR image of the right foot shows curvilinear hypointense trabecular fracture lines in the base of the fourth metatarsal (*arrow*). (**d**) Sagittal fat-suppressed T2-W MR image of the right foot shows associated marrow edema (*asterisk*). With the presence of a concordant history, the findings were consistent with a stress injury. (**e**) Frontal radiograph of the right foot in another patient at a later stage in the natural progression of a stress injury shows typical periosteal reaction adjacent to the neck of the second metatarsal (*arrowhead*), indicating a healing stress fracture. This is the earliest radiographic feature of stress injury

appreciate. This is especially so early in the course of destructive processes (e.g., osteomyelitis or osseous metastasis) or when fractures are undisplaced (e.g., hip fracture in the elderly adult) (Figs. 1.28 and 1.30).

Conclusion

Radiography as an imaging modality has inherent limitations in the demonstration of lesions involving soft tissues, as well as early in the course of abnormalities involving bone. Pitfalls

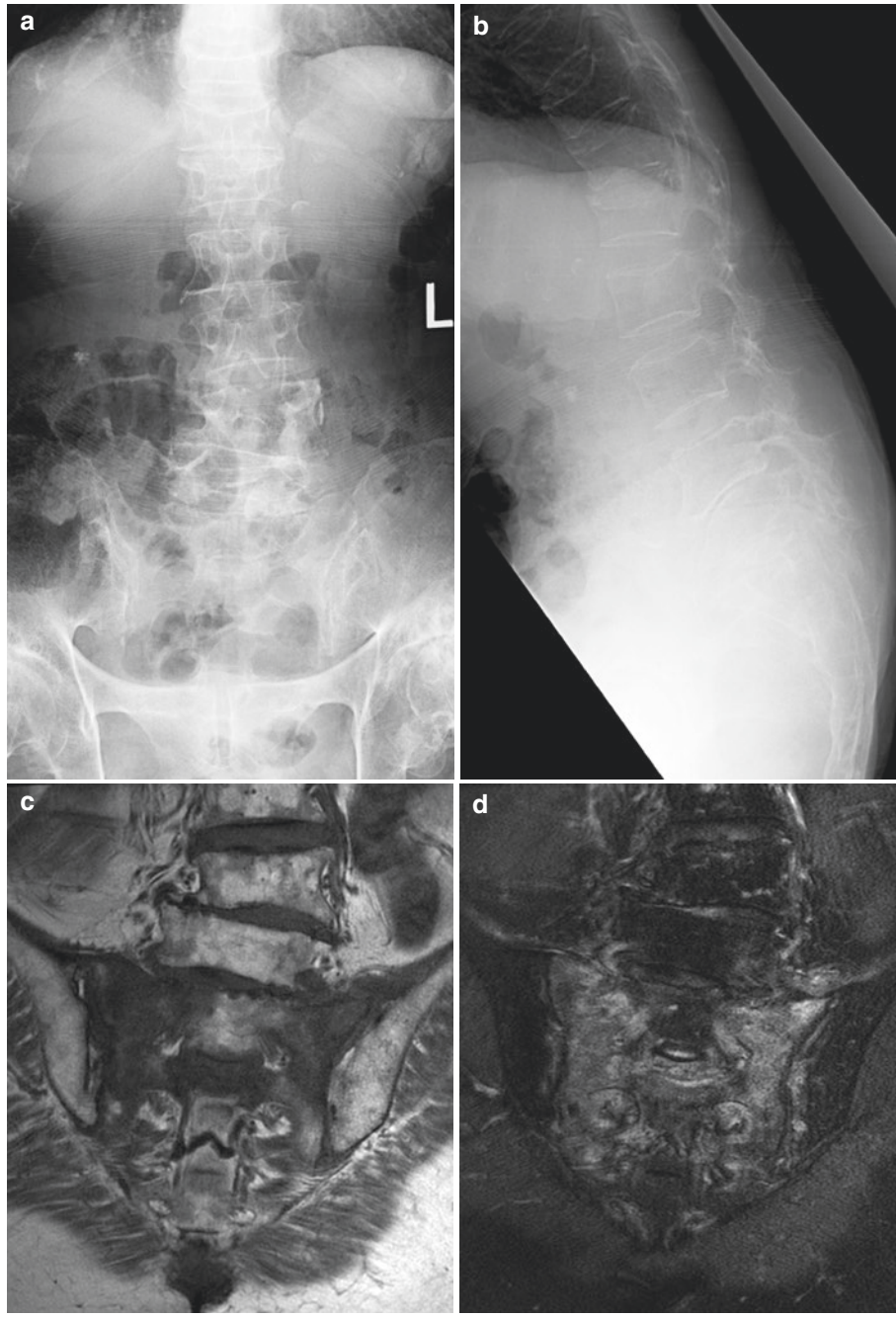

Fig. 1.30 A 74-year-old woman who presented with low back pain and tenderness in the upper gluteal region after a fall. (**a**) Frontal and (**b**) lateral radiographs of the lumbar spine show diffuse reduction in bone density consistent with osteoporosis. Known chronic osteoporotic compression fractures are seen at the thoracolumbar junction levels. Background spinal degenerative changes are evident, especially at the lower lumbar spine. (**c**) Coronal T1-W and (**d**) coronal fat-suppressed T2-W MR images of the sacrum show sacral insufficiency fractures, evident as a typical "H" pattern of T1-hypointense and T2-hyperintense marrow edema involving the bilateral sacral ala and the body of the second sacral segment. This finding is radiographically occult

are also encountered in radiographic acquisition, and if the clinician or radiologist is not cognizant of them, suboptimal diagnosis and patient management can ensue. Nevertheless, the humble radiograph remains a mainstay of diagnostic imaging in the modern day, frequently being the first-line imaging modality or assuming a complementary role to other more advanced imaging modalities.

References

Algra PR, Bloem JL, Tissing H et al (1991) Detection of vertebral metastases: comparison between MR imaging and bone scintigraphy. Radiographics 11:219–232

Aras MH, Miloglu O, Barutcugil C et al (2010) Comparison of the sensitivity for detecting foreign bodies among conventional plain radiography, computed tomography and ultrasonography. Dentomaxillofac Radiol 3:72–78

Blackburn WD, Bernreuter WK, Rominger M et al (1994) Arthroscopic evaluation of knee articular cartilage: a comparison with plain radiographs and magnetic resonance imaging. J Rheumatol 21:675–679

Ching W, Robinson J, McEntee M (2014) Patient-based radiographic exposure factor selection: a systematic review. J Med Radiat Sci 61:176–190

Crema MD, Roemer FW, Marra MD et al (2011) Articular cartilage in the knee: current MR imaging techniques and applications in clinical practice and research. Radiographics 31:37–61

Epner RA, Bowers WH, Guilford WB (1982) Ulnar variance – the effect of wrist positioning and roentgen filming technique. J Hand Surg Am 7:298–305

Eschler A, Rosler K, Rotter R et al (2014) Acromioclavicular joint dislocations: radiological correlation between Rockwood classification system and injury patterns in human cadaver species. Arch Orthop Trauma Surg 134:1193–1198

Fan YL, Peh WCG (2016) Radiology of osteoporosis: old and new findings. Semin Musculoskelet Radiol 20:235–245

Fife RS, Brandt KD, Braunstein EM et al (1991) Relationship between arthroscopic evidence of cartilage damage and radiographic evidence of joint space narrowing in early osteoarthritis of the knee. Arthritis Rheum 34:377–382

Gartner L, Pearce CJ, Saifuddin A (2009) The role of the plain radiograph in the characterisation of soft tissue tumours. Skelet Radiol 38:549–558

Gill SK, Smith J, Fox R, Chesser TJS et al (2013) Investigation of occult hip fractures: the use of CT and MRI. Sci World J 2013:830319

Gold RI, Seeger LL, Bassett LW, Steckel RJ et al (1990) An integrated approach to the evaluation of metastatic bone disease. Radiol Clin N Am 28:471–483

Gold GE, Chen CA, Koo S et al (2009) Recent advances in MRI of articular cartilage. AJR Am J Roentgenol 193:628–638

Guglielmi G, Muscarella S, Bazzocchi A (2011) Integrated imaging approach to osteoporosis: state-of-the-art review and update. Radiographics 31:1343–1364

Harris WH, Heaney RP (1969) Skeletal renewal and metabolic bone disease. N Engl J Med 280:193–202

Holmes JF, Akkinepalli R (2005) Computed tomography versus plain radiography to screen for cervical spine injury: a meta-analysis. J Trauma 58:902–905

Jarraya M, Hayashi D, Roemer FW et al (2013) Radiographically occult and subtle fractures: a pictorial review. Radiol Res Pract 2013:370169

Kijowski R, Blankenbaker D, Stanton P et al (2006) Arthroscopic validation of radiographic grading scales of osteoarthritis of the tibiofemoral joint. AJR Am J Roentgenol 187:794–799

Lee SK, Desai H, Silver B et al (2011) Comparison of radiographic stress views for scapholunate dynamic instability in a cadaver model. J Hand Surg Am 36:1149–1157

Liong SY, Whitehouse RW (2012) Lower extremity and pelvic stress fractures in athletes. Br J Radiol 85:1148–1156

Malik AK, Shetty AA, Targett C, Compson JP (2004) Scaphoid views: a need for standardisation. Ann R Coll Surg Engl 86:165–170

McCarthy EF, Sundaram M (2005) Heterotopic ossification: a review. Skelet Radiol 34:609–619

Murphey MD, Quale JL, Martin NL et al (1992) Computed radiography in musculoskeletal imaging: state of the art. AJR Am J Roentgenol 158:19–27

Ng WHA, Griffith JF, Hung EHY et al (2011) Imaging of the anterior cruciate ligament. World J Orthop 2:75–84

Oka M, Monu JUV (2004) Prevalence and patterns of occult hip fractures and mimics revealed by MRI. AJR Am J Roentgenol 182:283–288

Osmond JD, Pendergrass HP, Potsaid MS (1975) Accuracy of 99mTC-diphosphonate bone scans and roentgenograms in the detection of prostate, breast and lung carcinoma metastases. Am J Roentgenol Radium Therapy, Nucl Med 125:972–977

Pankovich AM (1976) Maisonneuve fracture of the fibula. J Bone Joint Surg Am 58:337–342

Pineda C, Espinosa R, Pena A (2009) Radiographic imaging in osteomyelitis: the role of plain radiography, computed tomography, ultrasonography, magnetic resonance imaging, and scintigraphy. Semin Plast Surg 23:80–89

Sankowski AJ, Lebkowska UM, Cwikla J et al (2013) The comparison of efficacy of different imaging techniques (conventional radiography, ultrasonography, magnetic resonance) in assessment of wrist joints and metacarpophalangeal joints in patients with psoriatic arthritis. Pol J Radiol 78:18–29

Seibold CJ, Mallisee TA, Erickson SJ et al (1999) Rotator cuff: evaluation with US and MR imaging. Radiographics 19:685–705

Shenoy R, Pillai A, Hadidi M (2007) Scaphoid fractures: variation in radiographic views - a survey of current

practice in the west of Scotland region. Eur J Emerg Med 14:2–5

Shetty CM, Barthur A, Kambadakone A et al (2011) Computed radiography image artifacts revisited. AJR Am J Roentgenol 196:37–48

Szkudlarek M, Klarlund M, Narvestad E et al (2006) Ultrasonography of the metacarpophalangeal and proximal interphalangeal joints in rheumatoid arthritis: a comparison with magnetic resonance imaging, conventional radiography and clinical examination. Arthritis Res Ther 8:R52

Takao M, Ochi M, Naito K et al (2001) Computed tomographic evaluation of the position of the leg for mortise radiographs. Foot Ankle Int 22:828–831

Taoka T, Mayr NA, Lee HJ et al (2001) Factors influencing visualization of vertebral metastases on MR imaging versus bone scintigraphy. AJR Am J Roentgenol 176:1525–1530

Theodorou DJ, Theodorou SJ, Kakitsubata Y (2012) Skeletal muscle disease: patterns of MRI appearances. Br J Radiol 85:e1298–e1308

Toth F, Sebestyen A, Balint L et al (2007) Positioning of the wrist for scaphoid radiography. Eur J Radiol 64:126–132

Walz-Flannigan A, Magnuson D, Erickson D, Schueler B (2012) Artifacts in digital radiography. AJR Am J Roentgenol 198:156–161

Ward RJ, Weissman BN, Kransdorf MJ et al (2013) ACR appropriateness criteria acute hip pain – suspected fracture. J Am Coll Radiol 11:114–120

Weiner SM, Jurenz S, Uhl M et al (2008) Ultrasonography in the assessment of peripheral joint involvement in psoriatic arthritis. Clin Rheumatol 27:983–989

World Health Organization (2003) Prevention and management of osteoporosis. World Health Organ Tech Rep Ser 921:1–164

Ultrasound Imaging Artifacts

2

Lana Hiraj Gimber and Mihra S. Taljanovic

Contents

Abbreviation

US Ultrasound

L.H. Gimber, MD, MPH
M.S. Taljanovic, MD, PhD, FACR (✉)
Department of Medical Imaging,
The University of Arizona College of Medicine,
Banner-University Medical Center,
1501 N. Campbell Avenue, P.O. Box 245067,
Tucson, AZ 85724, USA
e-mail: lgimber@radiology.arizona.edu;
mihrat@radiology.arizona.edu

2.1 Introduction

Ultrasound (US) imaging is an accessible imaging modality that does not employ ionizing radiation. However, while US imaging is easily employed, it is also very operator dependent. In clinical practice, the US beam often deviates from the ideal physical assumptions, and artifacts are created which can be mistaken for pathology. Artifacts can be found in both B-mode gray-scale and Doppler imaging. It is therefore important to be able to identify these artifacts and to employ techniques that can help avoid or minimize them.

2.2 Ultrasound Imaging

2.2.1 Equipment

US imaging employs the use of a small transducer, or probe, and US gel which is placed directly onto the skin. The probe transmits sound waves through the gel, which acts as a coupling medium, and into the body. Once in the body, the sound waves bounce off structures and return back to the probe. The computer then uses these collected sound waves to create an image. The US transducer contains thin piezoelectric crystals, which allow electrical signal to be converted to ultrasonic waves and the returning ultrasonic waves back into electrical signal (Smith and Finnoff 2009). There are different

W.C.G. Peh (ed.), *Pitfalls in Musculoskeletal Radiology*, DOI 10.1007/978-3-319-53496-1_2

frequency transducers. A transducer that has a lower frequency is often used to assess deeper structures but will however have a lower spatial resolution (Smith and Finnoff 2009). A transducer that has a higher frequency will not penetrate into the deeper tissues but will have a higher spatial resolution. In musculoskeletal US, a small footprint high-frequency linear (hockey stick) transducer is often used. This transducer accommodates small and curved surfaces and enables excellent evaluation of the superficial soft tissues.

2.2.2 Physics

Ultrasound is based on ideal physical beam assumptions. In the ideal situation, the US beam is assumed to travel in a straight line. As the US beam travels through tissues, it is assumed that the attenuation of sound is uniform. The speed of sound is assumed to be the same in all tissues. Once the US beam reaches an object, it is assumed that each reflector produces only a single echo. The echoes that are detected by the transducer are assumed to have originated from the main US beam. The depth of an object is directly related to the amount of time it takes the US echo to return to the transducer (Nilsson 2001; Feldman et al. 2009).

In clinical practice, the US beam deviates from these assumptions quite frequently. In addition to the main US beam, secondary beams outside of the main beam called side lobes and grating lobes are also created. Maximum sound wave reflection occurs when the sound wave is directly proportional to the imaged structure, which is not always possible to obtain. In addition, some sound waves are reflected back at the skin surface, while others can be absorbed in the examined tissues. When there is deviation from the ideal physical assumptions, artifacts are produced. These artifacts occur due to inherent characteristics of the US beam, errors in velocity, errors in attenuation, and presence of multiple echo paths (Feldman et al. 2009; Taljanovic et al. 2014).

2.2.3 Doppler US

Doppler US imaging was named after Christian Johann Doppler, an Austrian mathematician and physicist who described the "Doppler effect" in 1842. He stated that the observed frequency of a wave depends on the relative speed of the source and the observer (Roguin 2002). In US imaging, the "Doppler effect" is the change of frequency in a wave when a source moves relative to the receiver (Pozniak et al. 1992; Rubens et al. 2006; Teh 2006). Color, power, and spectral Doppler imaging enhance the traditional standard brightness mode (B-mode) gray-scale imaging and allow detection of vessels or abnormal blood flow in injured or pathologic tissues.

Color Doppler US produces an image that shows the presence, direction, and velocity of blood flow (Teh 2006). The image is superimposed on the gray-scale image. The differences in color on the image designates whether the flow is headed toward or away from the transducer. In addition, the mean velocity of the blood flow is color coded. Power Doppler US does not provide flow velocity and directional information. However, it has increased flow sensitivity and better vascular delineation (Martinoli et al. 1998). Power Doppler US displays the strength or power of the signal by measuring the amount of red cells passing by the beam (Martinoli et al. 1998; Teh 2006). The intensity of the blood flow is indicated by the color on the image. Spectral Doppler US interrogates a small region of a vessel, called a sample volume, and creates a spectral Doppler waveform (Rubens et al. 2006). This gives a quantitative analysis of the velocity and direction of blood flow (Teh 2006).

2.2.4 Normal Structures

Knowledge of the appearance of normal structures on US images is a prerequisite, before being able to identify US artifacts. Normal cortical bone (Fig. 2.1a) is hyperechoic and demonstrates posterior acoustic shadowing secondary to its highly reflective surface. Normal muscle (Fig. 2.1b) is hypoechoic with fine hyperechoic

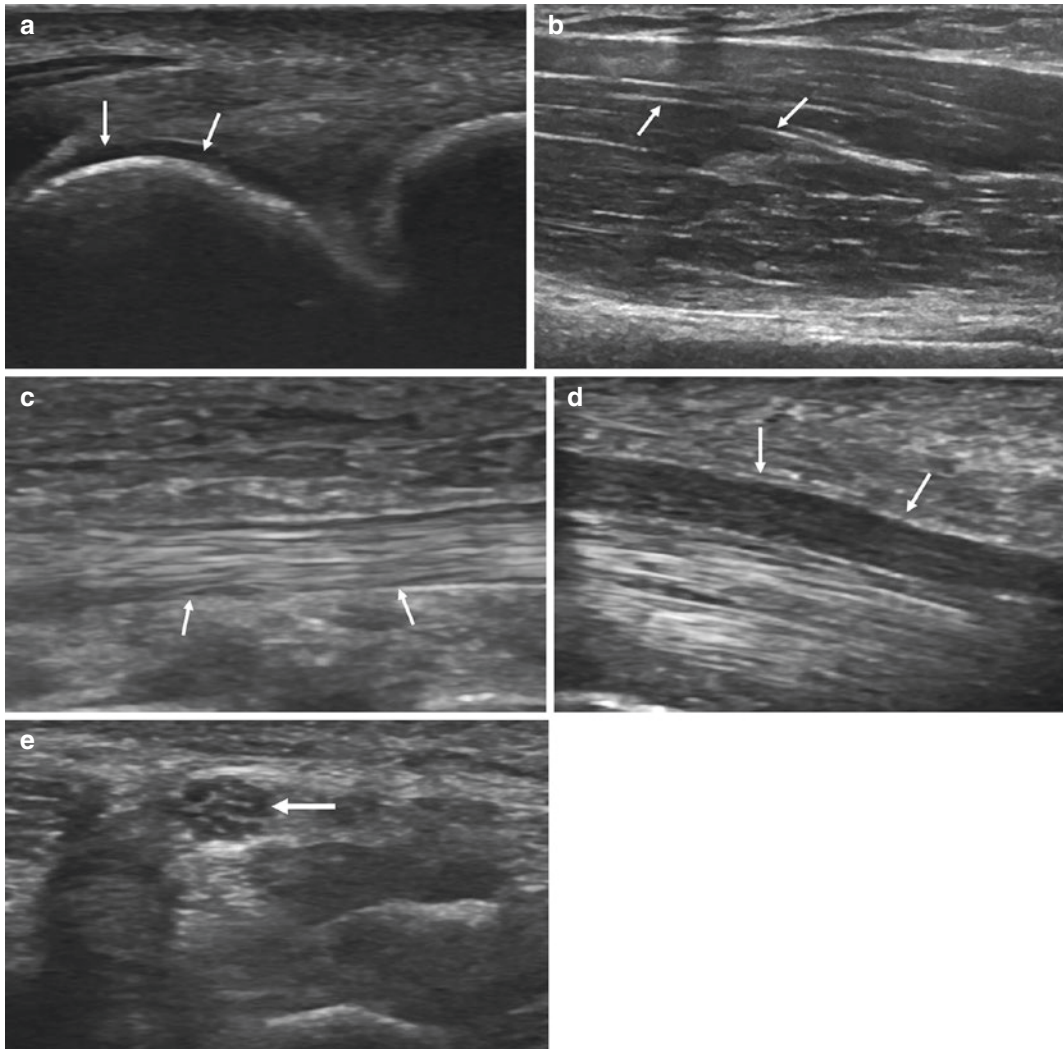

Fig. 2.1 Normal US imaging features of the musculoskeletal tissues. (**a**) Cortical bone at the metacarpophalangeal joint – normal hyperechoic cortical bone (*arrows*) with dirty posterior acoustic shadowing. (**b**) Muscle – normal pectoralis major muscle with hypoechoic muscle bundles separated by fine hyperechoic fibroadipose septa (*arrows*). (**c**) Tendon – normal posterior tibialis tendon (*arrows*) with echogenic fibrillar echotexture. (**d**) Normal peripheral nerve in the long axis – normal median nerve (*arrows*) with a fascicular architecture and appearing hypoechoic compared to adjacent tendon. (**e**) Normal peripheral nerve in short axis – normal median nerve with a speckled or honeycomb cross-sectional appearance (*arrow*)

fibroadipose septa separating the muscle into bundles. Normal tendon (Fig. 2.1c) is hyperechoic when compared to muscle and has a fibrillar echotexture. Normal nerve (Fig. 2.1d) can be hyperechoic relative to muscle or hypoechoic relative to tendon. The cross-sectional appearance of a normal nerve demonstrates a honeycombed or speckled architecture (Fig. 2.1e).

2.3 Gray-Scale Artifacts

2.3.1 Beam Characteristics

Artifacts related to intrinsic characteristics of the US beam are side-lobe, beamwidth, and anisotropy. Side-lobe artifacts create low-level spurious